

FOR REFERENCE

NOT TO BE TAKEN FROM THIS ROOM

LOAD TRANSFER MECHANISM
OF LATERALLY LOADED PILES

A MODEL STUDY

RIAD TAHA

Bogazici University Library



39001100314320

14

JUNE 1986

BOĞAZIÇI UNIVERSITY

LOAD TRANSFER MECHANISM
OF LATERALLY LOADED PILES
A MODEL STUDY

by

Riad TAHA

B.s. in C.E., U.S.I.U, Sandiago, Calif, 1982

Submitted to the institute for Graduate Studies in Science and
Engineering in partial fulfillment of the requirements for the
degree of

Master of Science
in
Civil Engineering

Boğaziçi University
1986

BOĞAZIÇI ÜNİVERSİTESİ
FEN BİLİMLERİ ENSTİTÜSÜ

RECORD OF COMPREHENSIVE EXAMINATION FOR MASTER'S DEGREE

DEPARTMENT : CIVIL ENG'G

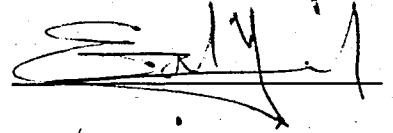
DATE : June, 26th, 1986

STUDENT : RIAD TAHA

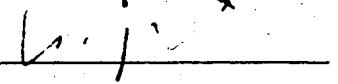
EXAMINATION COMMITTEE :

DOÇ.DR.EROL GÜLER

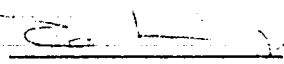
"THESIS SUPERVISOR"



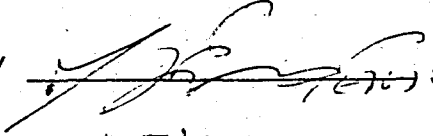
PROF.DR.ERGÜN TOĞROL



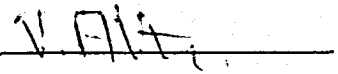
DOÇ.DR.TURAN H.DURGUNOĞLU



DOÇ.DR.TURGUT ERSOY



DOÇ.DR.VURAL ALTIN



RESULT OF EXAMINATION : PASSED

FAILED

C.E., CHAIRMAN

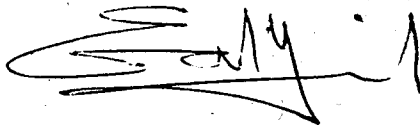




TABLE OF CONTENTS

	<u>Page</u>
- ACKNOWLEDGEMENT	I
- ABSTRACT	II
- ÖZET	III
- LIST OF FIGURES	IV
- LIST OF TABLES	V
- LIST OF SYMBOLS	VI
- CHAPTER ONE	
INTRODUCTION	1
- CHAPTER TWO	
SINGLE PILES : -	
2-1 Introduction	2
2-2 Ultimate load capacity of single piles	2
2-3 Laterally loaded single vertical piles	12
2-4 Pile load test	14
2-5 Constant rate of penetration (C.R.P)	14
2-6 Model Piles	15
2-7 Piles instrumentation	16
2-8 The test model pile	16
- CHAPTER THREE	
THEORY OF STRAIN GAUGE :-	
3-1 Introduction	18
3-2 Fundamentals of strain gauge technique	18
3-3 Construction of a strain gauge	18

	<u>Page</u>
- CHAPTER FOUR :	
TESTING METHOD : -	
4-1 Introduction.	25
4-2 Test equipment	25
4-3 Test pile.	27
4-4 Driving mechanism	27
4-5 Soil characteristics.	32
4-6 Testing program	35
- CHAPTER FIVE :-	
EVALUATION OF TEST RESULTS :-	
5-1 Data Processing	42
5-2 Analysis of data	45
- CHAPTER SIX : -	
SUMMARY AND CONCLUSIONS	63
- REFERENCES	65
- APPENDIX A	
INITIAL PILE DESIGN	67
- APPENDIX B	
TEST RESULTS	70
- APPENDIX C	77

Solutions of laterally loaded piles using finite element method.

ACKNOWLEDGEMENT

I would like to express my sincere gratitude to Doç.Dr. EROL GÖLER, for his invaluable suggestions, guidance, encouragements through the course of my study and especially in evaluation of test results.

RIAD TAHA

ISTANBUL, JUNE 1986

ABSTRACT

This study is concerned with the behavior of a model pile, embedded in cohesive soil and subjected to both vertical and lateral loads. Strains, due to both vertical and lateral loading, and lateral deflections are measured. The effect of repetitive lateral loading on lateral deflections, moments and load distribution along the pile is studied.

ÖZET

Bu çalışmada kohezyonlu zemin içersinde yatay ve düşey yüklere maruz bir model kazığın davranışı incelenmiştir. Düşey ve yatay yüklerden dolayı oluşan birim deformasyonlar ölçülmüştür. Tekrarlı yatay yüklerin, yatay deformasyonlar moment dağılımı ve kayak boyuncaki düşey gerilme dağılımı incelenmiştir.

LIST OF FIGURES

	<u>Page</u>
Fig 2-1 Pile bearing capacity components	4
Fig 2-1A The zones of shear beneath a shallow foundation according to Terzaghi	5
Fig 2-1B The zones of shear around the base of pile according to Meyerhof	6
Fig 2-2 Deflected forms of long and short piles acted upon by a horizontal force (Broms 1965)	13
Fig 3-1 Load cell "Full bridge arrangement"	20
Fig 3-2 Strain gauge positions for the measuring of normal stress	21
Fig 3-3 Standard strain gauge	22
Fig 3-4 Quarter bridge arrangement with compensating gauge	24
Fig 4-1 Details of test apparatus	26
Fig 4-2 Details of test pile	28
Fig 4-3 Strain gauge locations on both sides of test pile	29
Fig 4-3A The test pile and wiring	30
Fig 4-4 Jacking the pile	31

	<u>Page</u>
Fig 4-5A Soil mixing apparatus	33
Fig 4-5B Soil compaction	34
Fig 4-6 Loading arrangement	38
Fig 5-1 Load-settlement relationship graph	46
Fig 5-2 Load distribution along the pile	48
Fig 5-2A Variation of unit skin resistance at 80 kg Loading	49
Fig 5-2B Load carried by tip and wall at various loading level.	50
Fig 5-3 Lateral load-deflection graph and the effect of cyclic loading	54
Fig 5-4 Effect of increasing load on moment, lateral load = 4 kg, vertical load=0kg	56
Fig 5-4A Effect of repeated lateral load on moment, vertical load = 0 kg Lateral load = 8 kg	57
Fig 5-5 Effect of cyclic lateral, load on moment, lateral load = 8 kg vertical load = 40 kg	59
Fig 5-6 Redistribution of load after lateral load applications	61
Fig C-1 Model pile solution by finite difference method	79
Fig C-2 Shear and moment diagram evaluated by finite difference method	82

LIST OF TABLES

	<u>Page</u>
Table 3-1 Technical data of strain gauge 120LY11	22
Table 4-1 Loading history of test pile no. 1	39
Table 5-1 Load carried at each Section of pile	51
Table 5-2 Effect of repeated lateral loading on load distribution	62
Table B-2 Load-settlement test result	71
Table B-3 Measured Strain along the shaft	72
Table B-4 Strain readings due to 4 kg and 8 kg lateral loading (vertical loading = 0 kg)	73
Table B-4 Strain readings due to 4 kg and 8 kg lateral loading (vertical loading = 30 kg)	74
Table B-4 Strain readings due to 4 kg and 8 kg lateral loading (vertical load = 40 kg)	75
Table 5-4 Lateral load deflections Results	76

CHAPTER I

INTRODUCTION

During the past thirty years important investigations using instrumented piles had lead to better understanding of the mechanism in which friction pile transfer load to the supporting soil, a process refered to as load "take-out", as well as to the resistance to lateral loads of pile supported foundations.

This thesis describes the behaviour of a 2-7 cm single model pile subjected to several combinations of vertical and lateral loads. The pile was jacked closed ended to a penetration of 35 cm in a homogeneous soft clay. The pile was intrumented with strain gauges to measure the load distribution during vertical loading and bending moments along the embedded shaft of the pile under lateral loading.

The loading system was intended to simulate a condition that an isolated single pile loaded vertically with its designed working load is subjected to repetitive lateral loading. An additional vertical load, equivalent to a possible over load, was then applied and the lateral load was cycled again, lateral deflections and moments distributions along the shaft are evaluated. The effects of the magnitude of the lateral loads and the number of lateral deflections and moment distribution are investigated. Load distribution along the shaft under selected compressive loads levels are evaluated as well. Finally, the effect of lateral loading on the distribution of load along the pile is discussed.

CHAPTER 2 SINGLE PILES

2.1 INTRODUCTION :

Piles are structural members (timber, concrete or steel) used to transmit surface loads from the super structure to lower levels in the soil stratum without risk of shear failure or excessive settlement. Piles are generally used, as a second solution, when the foundation soil is not suitable for the use of shallow foundations.

Piles are classified in many ways, according to their function (end bearing, friction piles), according to their use (tension, batter, anchor) or according to their method of installation (replacement : driven piles and jacked piles).

This chapter will be concerned with the static analysis methods for pile capacity, the computation of vertical and lateral load capacities and the procedures used in load tests. Pile instrumentations, and the theory behind pile modeling is briefly discussed.

2-2 ULTIMATE LOAD CAPACITY OF SINGLE PILES :

The analysis of bearing capacity of single piles from measured soil properties is based on the so - called "static approach", in which the following factors are responsible for the load-carrying capacity of a pile :-

- 1- As the base of a pile is pressed downward by a load on the head, the soil immediately below and to the sides of the base must be pushed aside. The soil offers a resistance to the shearing action which such a movement entails.
- 2- Downward Movement of the pile relative to the soil surrounding causes the mobilisation of tangential forces on the shaft surface that oppose motion. These values are due both to adhesion and to the friction of the soil on the shaft surface (Fig 2.1).
- 3- The pile takes the place of a certain volume of soil, the weight of which was previously carried by the soil below the base of the pile. It is assumed that the weight of pile is equal to the weight of soil replaced.

Taking the above factors into account, the ultimate load capacity of the pile $(Q)_{ult}$, is evaluated as the sum of two components, the ultimate pile capacity carried by the point in end bearing $(Q_p)_{ult}$, and the ultimate pile capacity carried by skin resistance $(Q_s)_{ult}$.

$$(Q)_{ult} = (Q_p)_{ult} + (Q_s)_{ult} \tag{2-1}$$

or

$$(Q)_{ult} = (q)_{ult} A_b + (f_s)_{ult} A_s \tag{2-2}$$

In the above equation, $(q_t)_{ult}$ and $(f_s)_{ult}$ represent the unit ultimate resistance of the point and the shaft respectively, their values may be calculated from measured soil properties, found experimentally or obtained from given empirical formulae's or charts.

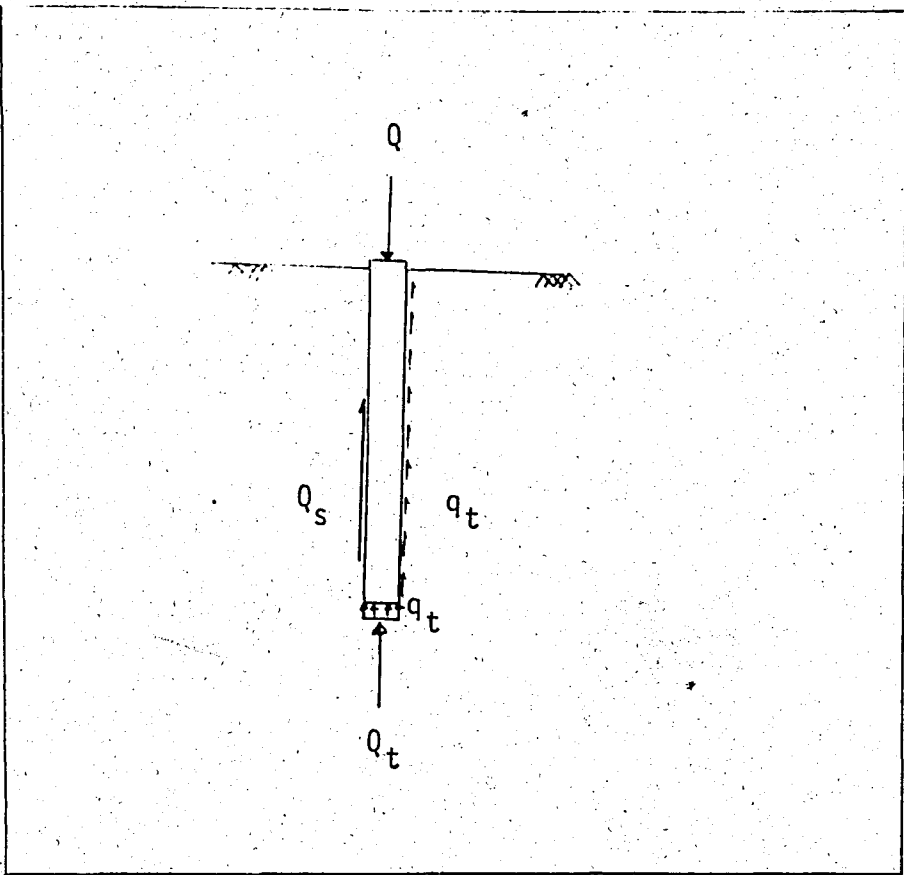


Fig. 2-1 Pile bearing capacity components

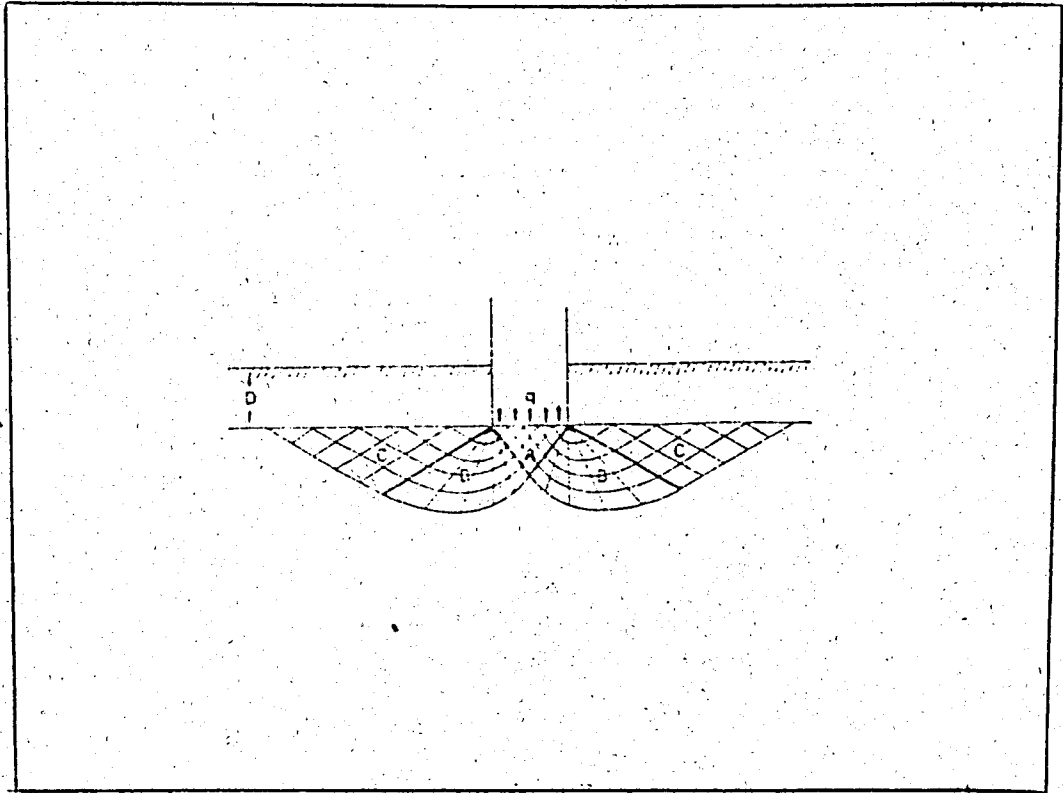


Fig.2-1A.The zones of shear beneath a shallow foundation according to Terzaghi.

- A,zone of elastic equilibrium,
- B,zones of radial shear,
- C,zones of passive shear.

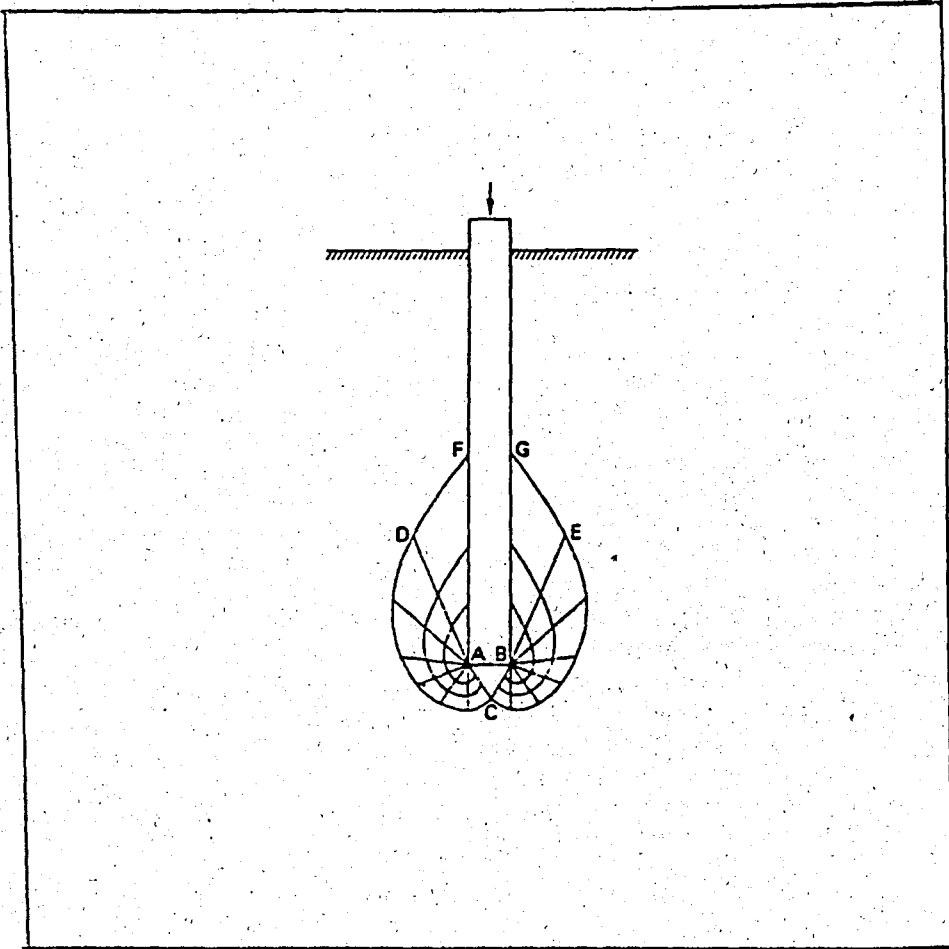


Fig.2-1B.The zones of shear around the base of a pile,
(according to Meyerhof)

Terzaghi, Meyerhof and others proposed various theoretical solutions for the two dimensional problem of bearing capacity and failure mechanism of single piles. Meyerhof expressed the ultimate unit base resistance as :

$$(q_t)_{ult} = CN_c + K_s j D N_q + j \frac{B}{2} N_j \quad (2-3)$$

where :

K_s = the coefficient of earth pressure on the shaft within the failure zone; varying from $\frac{1}{2}$ for loose soil to about 1 for dense soil

C = cohesion of the soil

(j) = the density of the soil

D = the length the pile

B = the breadth of the pile

N_c, N_q, N_j = bearing capacity factors that are dependent on the embedment ratio D/B .

In a soil, giving both adhesion and friction on the shaft of the pile, Meyerhof (1953) expressed the ultimate unit resistance of shaft as :

$$(f_s)_{ult} = C_a + K_s j D \tan(\delta) \quad (2-4)$$

where:

C_a = the adhesion per unit area

δ = the angle of friction of the soil on the shaft.

ULTIMATE BEARING CAPACITY OF SINGLE PILES IN CLAY : -

For piles in clay, the undrained capacity is generally taken to be the critical value "total stress analysis", unless the clay is highly over - consolidated then, the "effective stress-drained" analysis proposed by Burland (1973) is more appropriate.

If the clay is saturated, the undrained angle of friction is zero, then $N_q = 1$, $N_{\phi} = 0$ and $K_s = 1$. resulting

$$(q_t)_{ult} = C_u N_c \quad (2-5)$$

also, $s = 0$ for clays, then

$$(f_s)_{ult} = C_a \quad (2-6)$$

Substituting equations (2-5) and (2-6) in equation (2-2) gives : -

$$(Q)_{ult} = C_u N_c A_b + C_a A_s \quad (2-7)$$

where :

C_u = Average undrained shear strength of the soil at the base of pile evaluated from tests on undisturbed samples of soil "Triaxial test"

N_c = Bearing capacity coefficient, it is taken to be equal to (9) for practical purpose "undrained conditions,

$$\phi_u = 0"$$

- C_a = Average adhesion between the pile and soil
 A_s = Surface area of embedded length of pile
 A_b = Area of the base :.

The average adhesion between pile and soil, C_a , is related to the undrained soil strength, C_u , by an adhesion factor α , such that :-

$$C_a = \alpha C_u \quad (2-8)$$

The α factor is determined by many researchers as the Tomlinson's method, Meyerhof's method and Vijayvergiya and Focht's method for driven piles and Tomlinson's, Skempton and Mohan and Chandra Methods for bored piles.

Substituting equation (2-7)

$$(Q)_{ult} = C_u N_c A_b + \alpha C_u A_s$$

Driven piles :

When a pile is driven into clay, shear surfaces associated with the base are progressively formed deeper and deeper in new soil as penetration proceeds. Around the shaft the soil is compressed and moved laterally and vertically to accommodate the pile, the ground surface heaves and the clay in the immediate vicinity of the pile shaft is completely remoulded. According to Casegrande (1932), the zone of remoulding has a diameter twice

the diameter of the pile and the soil is sufficiently affected within a zone four times the pile diameter to cause an increase in compressibility. If the clay is sensitive, there is an immediate loss in strength due to remoulding, and in both sensitive and non-sensitive unfissured clay there is an increase in pore water pressure in the compressed zone. In the period following driving, pore pressure dissipation and the drainage may be sufficient to restore the strength, this phenomenon is called "take up" and in some soils the bearing capacity of a pile relying chiefly on shaft friction, may increase to many times its value immediately following driving.

In most cases the increase of bearing capacity with time is rapid at first, so that by the end of a month the ultimate bearing capacity is not much less than which would be reached in a year or more. Peck (1958) concluded that in soft and medium clays, having unconfined compressive strengths up to about 96 KN/m^2 the contribution made by shaft friction to the ultimate bearing capacity, after a period for "take up" was equal to the product of the embedded area and the original shearing strength of the soil. The shearing strength was taken to be half the unconfined compressive strength of undisturbed samples. Thus, for soft clays $f_u = C$ for design purposes. In the case of piles driven into stiff clays, Peck found that the shaft resistance was smaller than the product of the embedded area and the shearing strength of the soil and that as the shear strength increased the difference became greater. Others have also noted this effect. Thus, for stiff clays $f_u < C$.

In the stiff fissured clays, it is possible that the displacement of the clay may break into blocks or fragments and the effect on pore pressure is not known.

2-3 LATERAL LOADED SINGLE VERTICAL PILES :

Piles are frequently subjected to lateral loads as well as vertical loads. Lateral loads may be due to wind forces on high buildings, traffic impact forces and wind forces on bridges, and lateral earth pressure. Wave and ship collisions on shore and off shore structures.

Under the action of horizontal load, the pile behaviour is largely governed by the pile length, head conditions (free or fixed) and the stiffness of pile and soil. In the case of a short pile failure will occur in the surrounding soil while in the case of a long pile failure of pile material might govern due to the fact that the stresses induced are higher than the allowable yielding stress of pile material. The deflected shapes of short and long piles under the action of horizontal force acting at the ground level is shown in Fig 2-2.

Solutions for the ultimate load capacity for short and long piles as well as evaluating the deflection at the top of the pile is given by Broms (2).

Bowels has introduced a finite elements solution for laterally loaded piles under various conditions.

It may be worth mentioning that the design of piles for lateral loading will be governed by a limiting allowable deflections that may result an allowable lateral load much less than the ultimate lateral load capacity of the pile since the

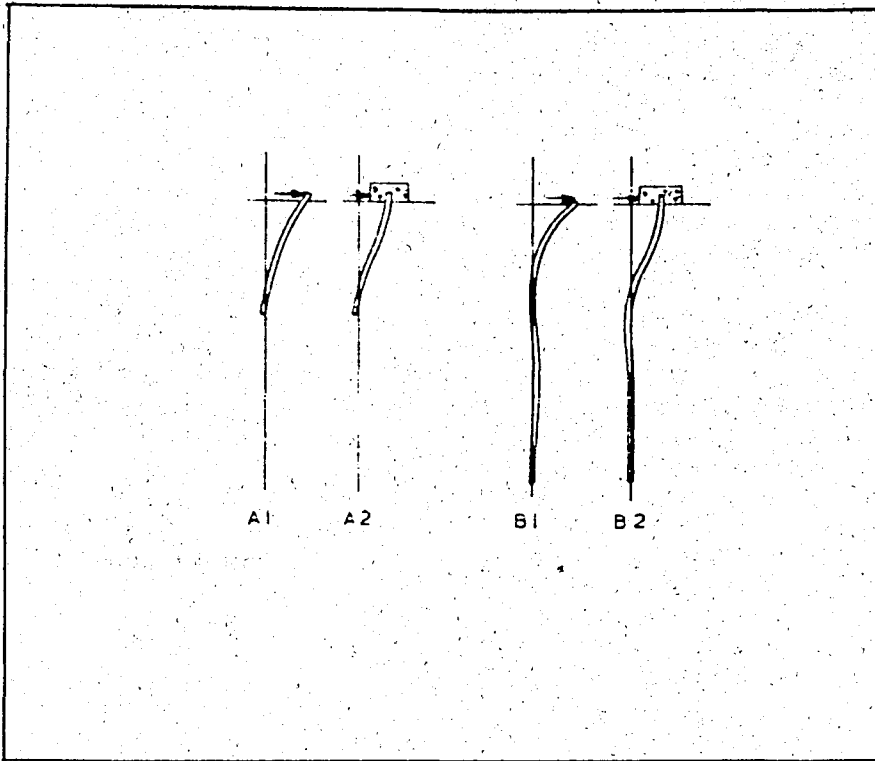


Fig. Deflected forms of long and short piles acted upon by a horizontal force. (Broms 1965)

A1: short pile with no head restraint:

A2: short pile with pile cap allowing no rotation;

B1: long pile with no head restraint;

B2: long pile with pile cap allowing no rotation

ultimate load may be reached at very large unsafe deflections.

2-4 PILE LOAD TESTS : -

pile load tests are carried out on single or group of piles for one or more of the following reasons : -

- 1- To determine the load-settlement relationship of pile.
- 2- To evaluate the ultimate load carrying capacity of pile and to check the calculated value in the initial design calculated from static or dynamic approach.
- 3- To check that the selected working load, evaluated from the ultimate load capacity divided by a factor of safety, is a satisfactory one.

Common types of pile load tests are compression tests, uplift tests and lateral tests. Many procedures of load tests are found in practice. In case of compression tests, the common procedures are :-

- 1- Maintained loading tests.
- 2- Constant rate of penetration (C.R.P) tests
- 3- Method of equilibrium.

Details of the procedures are given by ASTM, local codes and procedures recommended by pioneers. Here we will only take a closer look to the C.R.P method.

2-5 CONSTANT RATE OF PENETRATION (C.R.P.)

This test was developed by Whitaker (1957) for model

piles and was latter used for Full-scale pile tests. In carrying out the C.R.P test, the pile is made to penetrate the soil at a constant speed from its position as installed, and the force applied at the top of the pile to maintain the rate of penetration is continuously measured. The soil supporting the pile is stressed under conditions approaching a constant rate of strain until it fails in shear and when this occurs the ultimate bearing capacity of the pile has been reached. The settlement is measured by means of dial gauge. The test is usually arranged to take about the same time as a laboratory undrained test on a sample of the soil to ensure that the undrained load capacity and the load-undrained settlement relationship are obtained.

The purpose of the C.R.P test is to determine the ultimate load capacity of the pile. The load-penetration curve obtained in the test doesn't represent an equilibrium relationship between load and settlement, so that the settlement to be expected under working conditions is not found. Pile movement should be regarded as necessary for mobilising the forces of resistance

2-6 MODEL PILES : -

Full scale pile load tests are expensive and time consuming tests, especially when the behaviour of a group of piles is investigated. As a solution to this problem, model tests under controlled lab conditions on scaled model piles, instrumented or uninstrumented, simulating certain conditions that may exist in practice is frequently used to find solutions suitable for practical design purposes.

Instrumented piles, singles or groups, are frequently used in practice, for full scale as well as model piles, in carrying out load tests and in investigations of piles behaviour under various loading conditions.

Electrical strain gauges fixed at certain locations along the embedded length of the pile is one method of pile instrumentations. The measured strains are used to evaluate the load distributions along the pile shaft under compression or tension loading. The difference in the loads at any two cross sections represents the load carried by friction or adhesion on the surface of the shaft between the two sections.

The load carried by the tip may be measured directly from a load cell, put at the end of the pile, or may be extrapolated from the resulted curves, from which the percentage of load carried by tip or and shaft are computed. Moment distribution along the shaft under lateral loading may be evaluated as well by converting the resulted strains to loads which is converted to moments at the strain gauges level.

Details of strain gauges, method of placing and measurements as well as the theory behind using strain gauges in experimental stress analysis is given in the proceeding chapter.

2-8 THE TEST MODEL PILE : -

In this study, a model instrumented vertical single pile

subjected to a combination of vertical compression and lateral loads is investigated. The pile is jacked in a homogenous cohesive soil and tested using the constant-rate-of penetration procedure.

The pile dimensions, instrumentation and the loading procedure as well as the soil conditions are presented in the following chapters.

The computed pile ultimate load capacity, the designed working load as well as the lateral loads acting on the model pile using the previous mentioned formulues are presented in Appendix A.

CHAPTER 3

THEORY OF STRAIN GAUGE

3-1 INTRODUCTION

In this chapter, the theory and application of strain gauges used in experimental stress analysis are discussed. A brief description of type, technical data of the strain gauges and measuring instruments used in carrying out the test are presented.

3-2 FUNDAMENTALS OF STRAIN GAUGE TECHNIQUES :

Electrical resistance strain gauges are used in experimental stress analysis which makes it possible to assess the stressing of a structural part within wide limits. The theory behind the strain gauge technique is that the strain gauge transforms strain applied to it into a proportional change of resistance. The relation between the applied strain ($\epsilon = \Delta l / l$) and the relative change of resistance of a strain gauge is described by the equation.

$$\frac{\Delta R}{R} = K \epsilon$$

where k is gauge factor, calibrated by the manufacturer for each package.

Figure 3-1 shows a load cell configuration in which four active strain gages are used in the measuring circuit (Full bridge arrangement).

Considering the prismatic bar in Fig 3-2 under axial load, the resistance R_1 and R_2 decrease owing to axial shortening of the element while resistance in R_3 and R_4 increases ($\epsilon_x = \mu \epsilon$). When the strain gauges are connected up in the wheatstone Bridge circuit, then as the element is compressed, the output measured between 1 and 3 will vary proportionally to the load applied.

3-3 CONSTRUCTION OF A STRAIN GAUGE : -

Figure 3-3 shows the principal construction of a standard strain gauge. Embedded between two plastic strips is the measuring grid, the active part of the gauge, and is made from a thin metal foil which is electrically conducting. Larger areas at the end of the grid facilitate the connection of cables. The separate layers of the gauge are bonded together. The plastic carrier or matrix helps to handle the gauge and protects the active grid against mechanical damage.

The strain gauge must be mounted on the surface of the specimen of which the stress shall be determined by means of special adhesives recommended by the manufacturer for each type of strain gauge.

In this work, a total of 11 HBM strain gauges type 6/120 LY 11 are used. The characteristic data dimensions of the strain gauge is given in the table 3-1

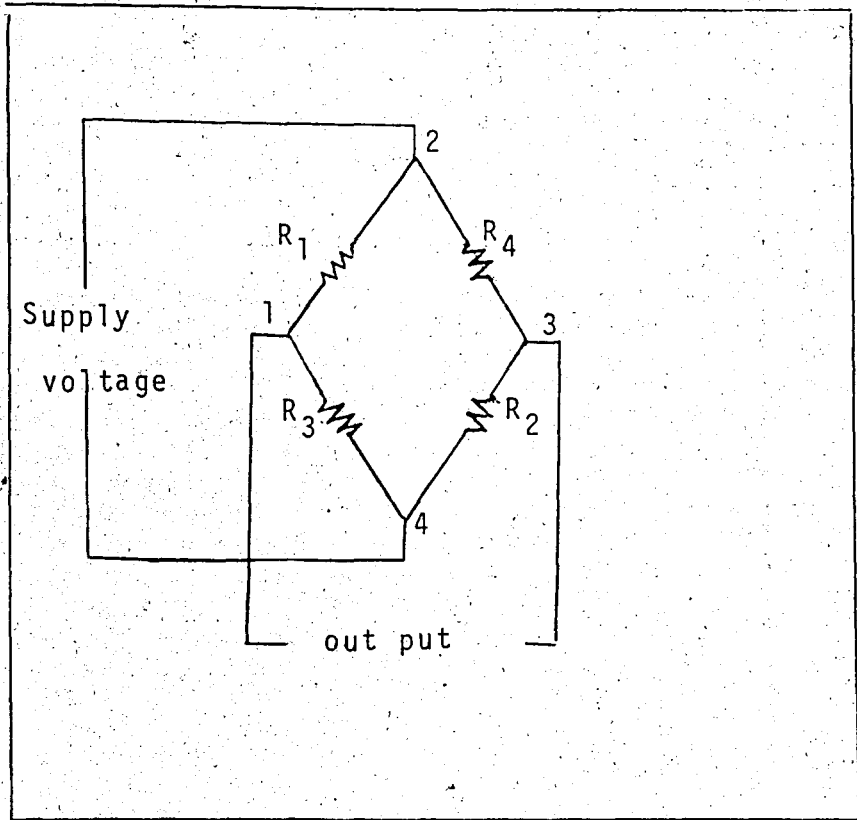


Fig. 3-1 Load cell "Full bridge arrangement".

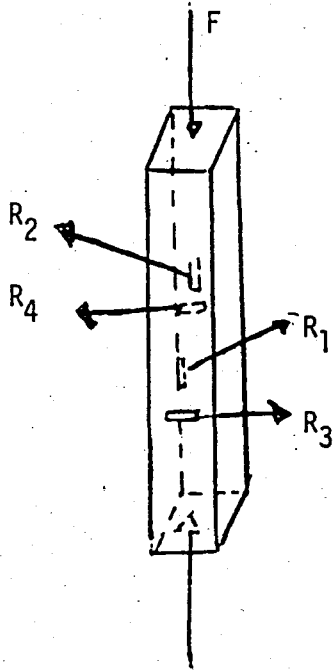


Fig. 3-2 Strain gauge Positions for the measuring of normal stress

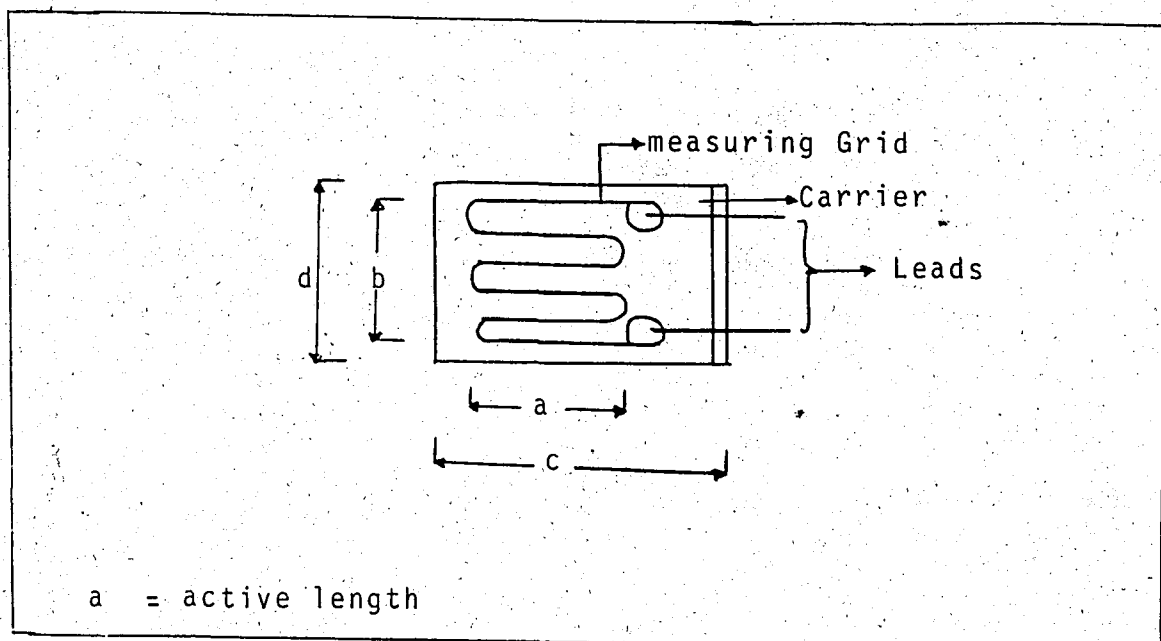


Fig.3-3 Standard strain gauge

Type	Nominal Resistance (ohm)	Dimensions				Maximum permitted bridge energizer voltage (Vrms)	Gauge Factor K	Service temp change static measurement C°
		Grid		Carrier				
		a	b	c	d			
6/120LY11	120	6	2.8	12.8	6.3	9	2.0 5	-70— +200

Table 3-1 Technical data of strain gauge b/120LY11

The strain gauges were fastened to the inside face of the model pile by means of HBM Rapid adhesive X-60. 4-wire HBM cable is used for leads in the three wire circuit employed. A quarter bridge with compensating gauge arrangement is used as shown in Fig 3-4

The dummy gauge and loads were maintained at the same temperature as the test pile to minimize temperature effect during testing. "drift" strain measurement is made by a SR4 - strain Indicator type N reading strain in the order of ($\epsilon \times 10^{-6}$ inch/inch). The procedure for strain gauge cementation, lead soldering and further information is given in H.BM publications. (5).

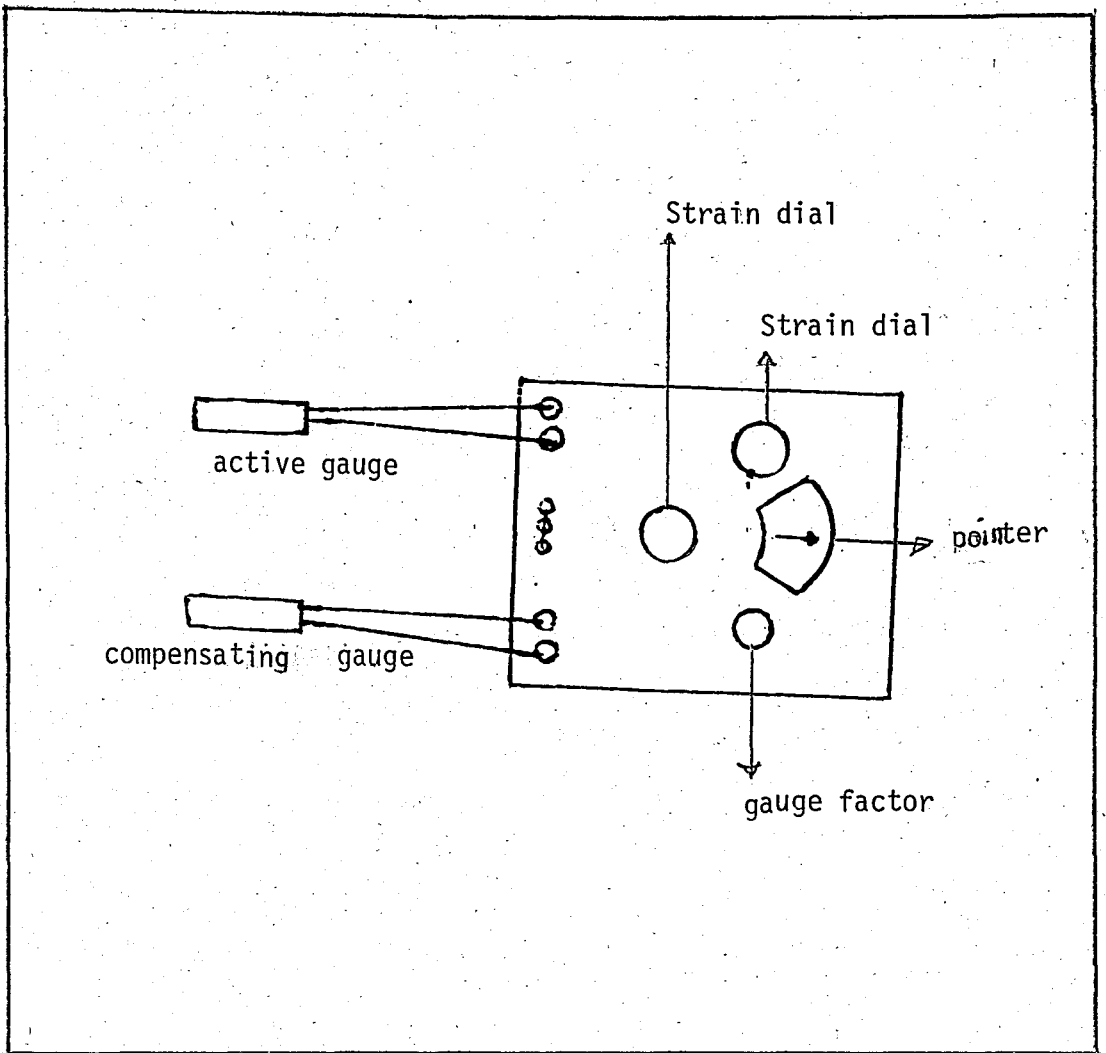


Fig.3-4 Quarter bridge arrangement with
Compensating gauge.

CHAPTER 4

TESTING METHOD

4-1 INTRODUCTION

In this chapter, details of the test equipment, soil characteristic and testing procedure are described. The loading system is designed to simulate a condition that, a single pile, loaded vertically with its design working load of 30 kg, is subjected to repetitive lateral loading. An additional vertical load of 10 kg, representing an equivalent design over load due to variation of life load, is then introduced and the lateral load is cycled again. The change in the load distribution, due to the repetitive lateral loading, along the shaft is investigated. Finally, lateral load is then cycled under zero vertical load to compare moments and deflections at the pile with zero vertical load.

4-2 TEST EQUIPMENT

Apparatus : -

The apparatus shown in Fig 4-1 was used in the test. Vertical loads were applied by means of a stepless compression machine at a slow rate of deformation, namely 0.40 mm/min. The vertical loads were measured by a load gauge mounted on top of the pile cap. Repeated lateral loads were applied by means of a string passing over a pulley. Pile top movement

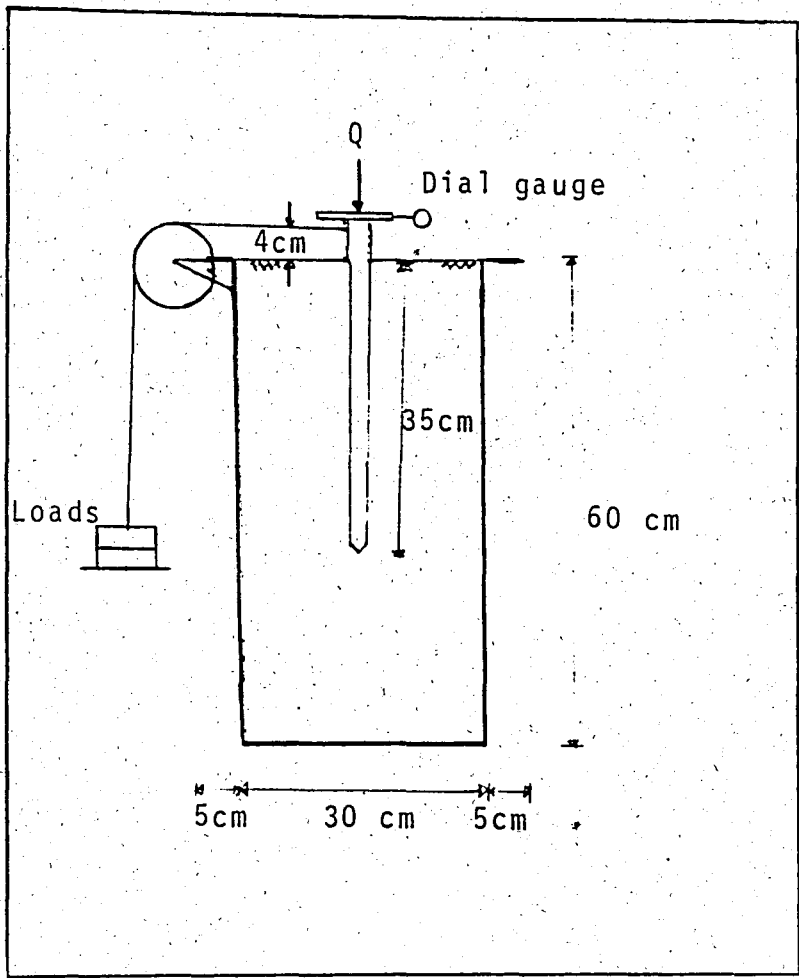


Fig. 4-1 Details of test apparatus

and lateral deflections were measured with dial indicators reading to 0.01 mm. Bearings were placed between the cap and the loading Frame to reduce friction during horizontal movement of pile head. The Steel container had a wall thickness of 8 mm, an internal diameter of 300 mm and a height of 600 mm. The small size of the container was due to the restricted size of the stepless compression machine. The inside surface of the container was greased to reduce wall friction between soil and container during pile driving.

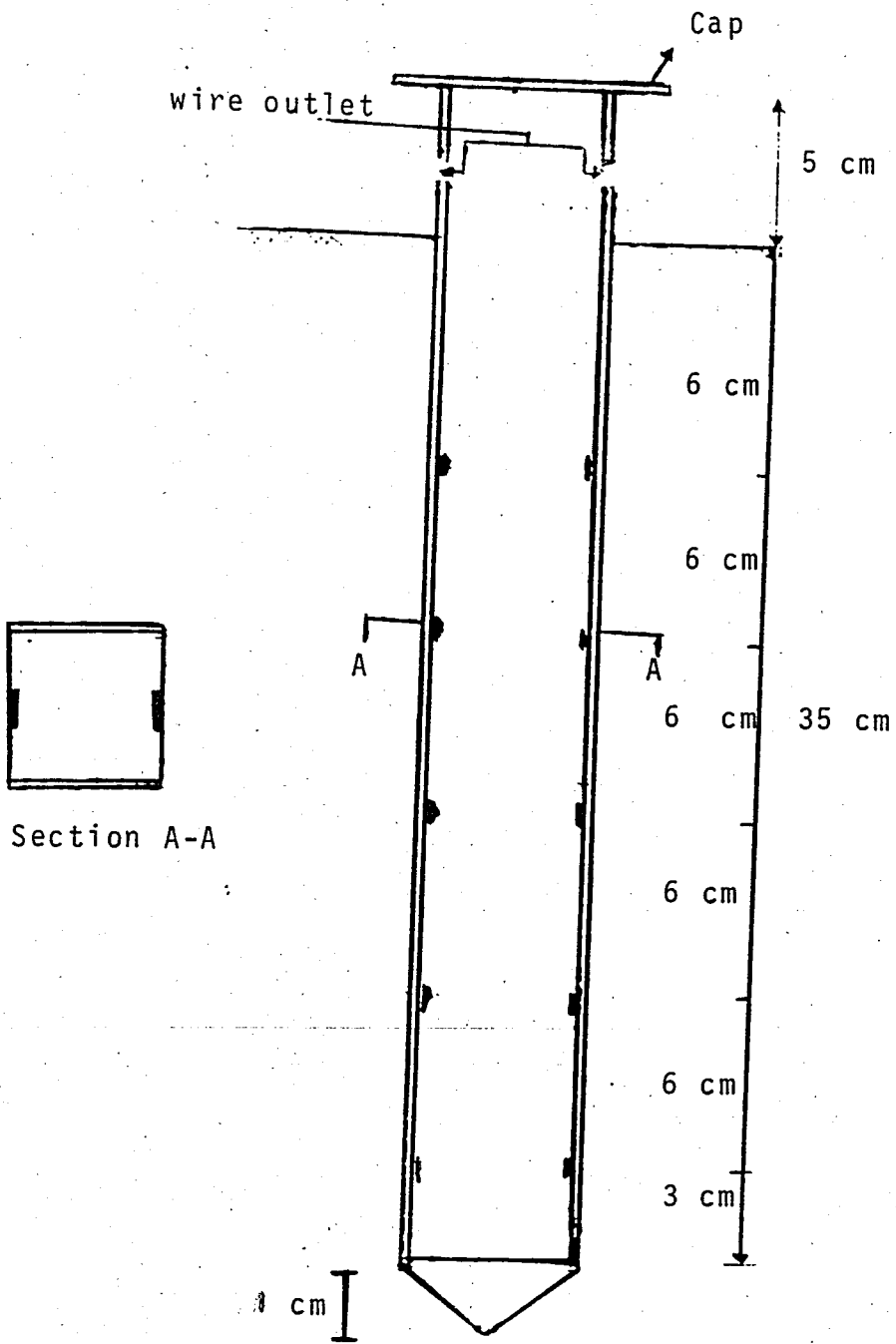
4-3 TEST PILE :-

Two identical square closed ended pipe model piles were fabricated from aluminium alloy. Each pile consists of two equal legged \sqsubset channels fastened by a brittle iron glue forming a square section, Fig 4-2. The external diameter was 27 mm, wall thickness 0.50 mm and the embedded shaft length was 350 mm. A total of 10 electrical resistive strain gauges were bonded on the internal surface one pile at 5 locations, one pair at each level as shown in Fig 4-3, forming a quarter bridge arrangement. The dummy compensating strain gauge was bonded on a separate sheet of aluminium and kept at the same temp and conditions as the test pile. The second pile was uninstrumented.

The test piles were fitted with a rigid steel cap placed on top of the pile head.

4-4 DRIVING MECHANISM :

The pile was jacked using a stepless compression.



Section A-A

Not to scale

Fig. 4-2 Details of test pile

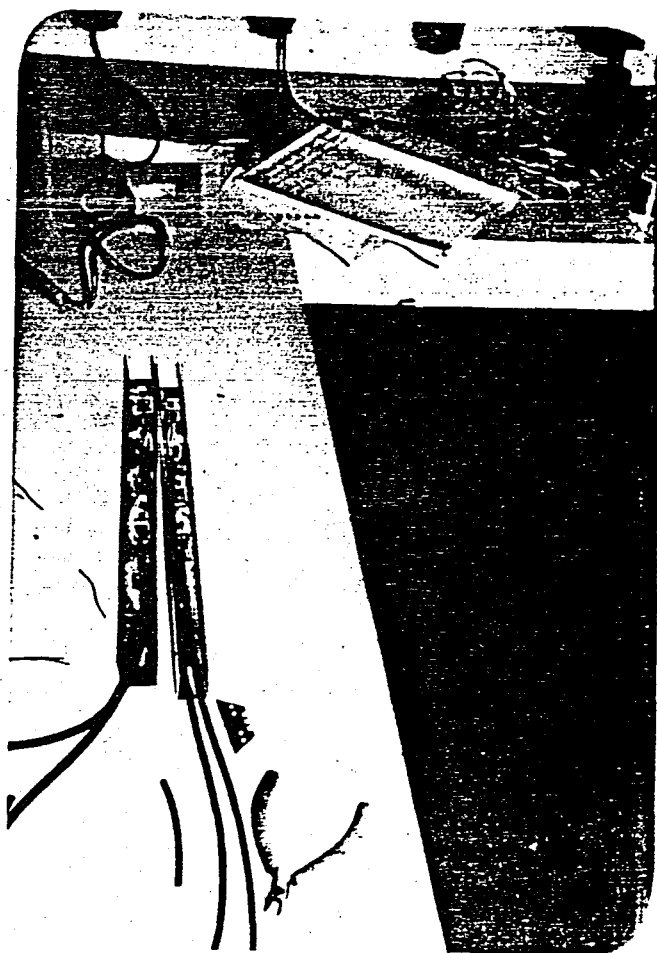


Fig. 4-3 Strain gauge locations on both sides of test pile



Fig. 4-3A The test pile and wiring



Fig. 4-4 Jacking the pile

machine. The rate of penetration was 2mm/min. The rate of penetration was chosen such that it causes a minimal disturbance to the surrounding soil and confirms with the rate of penetration used in practice in jacking full scale piles insitue. The time taken for driving the test pile, 350 mm, was approximatly 3 hours. The soil surface arround the pile was covered with athin layer of water to lubricate any gap formed between the pile and the soil during driving.

The pile was loaded 24 hours after driving to assure the dissipation of excess pore-water pressure that might have developed during driving.

4-5 Soil Characteristics :-

The soil used in the test was taken from a site near KILYOS USKUMRU KÖY, which consists of a clay passing through the no 200 seive. The liquid limit is 69 % and the plastic limit is 29 %. The optimum water content is 25 %. The soil was compacted in thin layers at near standard proctor energy at water content several percents higher than the optimum water content in order to achieve high degree of saturation and near Uniformity in strength. The average water content to a depth of 40 cm was 33 %. The soil was subjected to 2 kg/cm² water pressure after compaction, for 24 hours to assure high degree of saturation

Unconsolidated-undrained triaxial compression tests were carried out on samples recovered from the test champer to evaluate the undrained shear strength of the soil . The

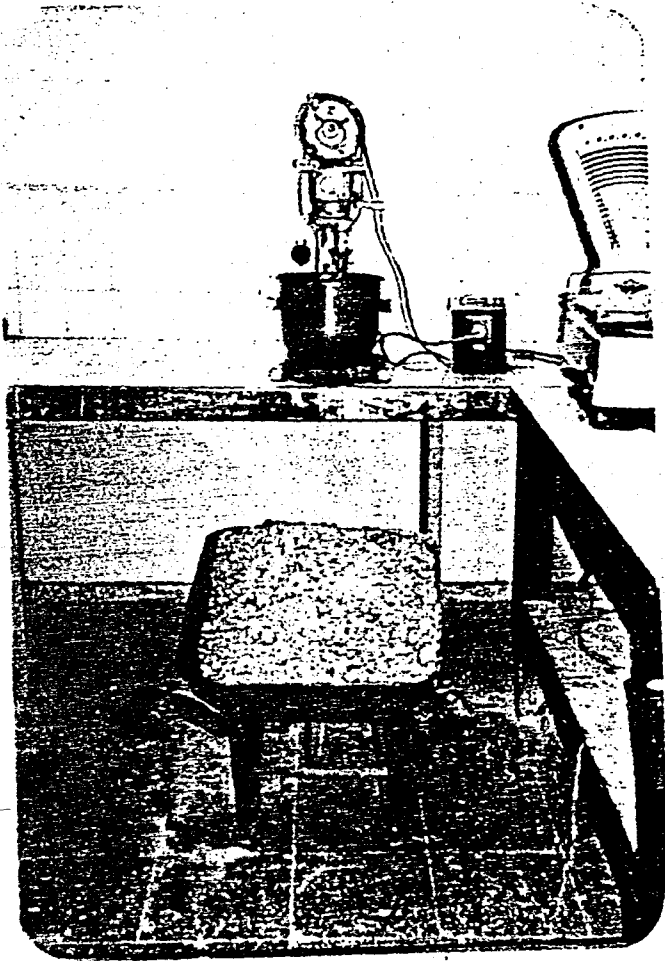


Fig. 4-5A Soil mixing Apparatus

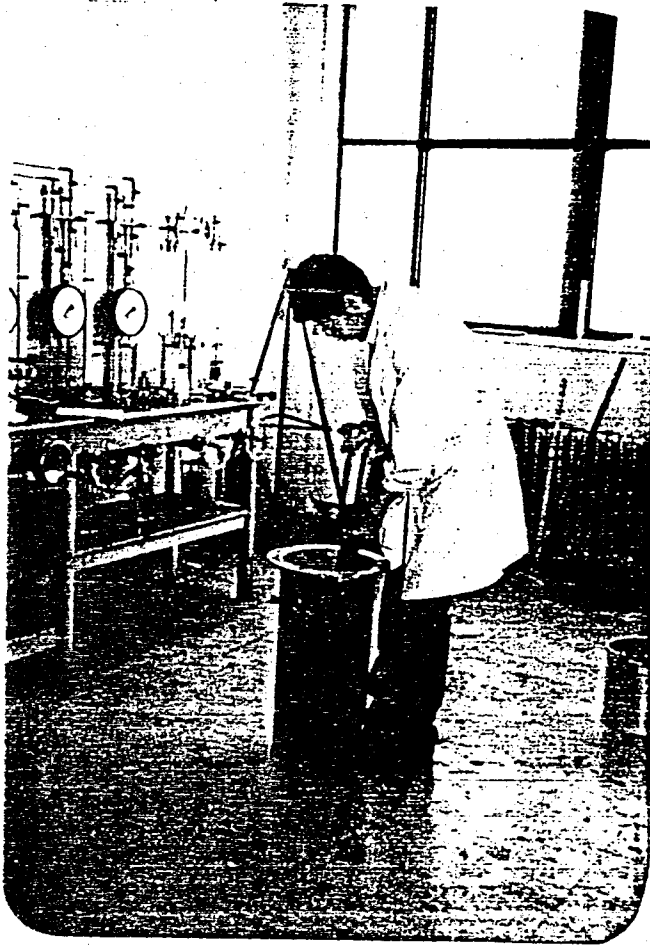


Fig. 4-5B Soil compaction

confinment pressures were 0, 0.5, 1.0 and 2.0 kg/cm². The measured value was :

$$C_u = 0.2 \text{ kg/cm}^2$$

Soil preparation steps are shown in Fig 4-5A and 4-5B
4-6 TESTING PROGRAM

Introduction : -

In this section, the detail of testing procedure is described. The loading system is designed to simulate a condition that a single pile loaded vertically with its designed working compressive load, 30 kg, is subjected to repetitive lateral load. An additional vertical load of 10 kg representing an equivalent design overload, due the variation of life load, is introduced and the lateral load is cycled again. Finally, the lateral load is cycled under zero vertical compressive load to compare moments and deflections.

Testing Procedure :-

A constant rate of penetration was followed in loading the pile vertically, 24 hours after driving, by means of a stepless compression test machine. The machine has a capacity of 5000 kg. The penetration speed was 0.0400 mm/min.

A total of two load tests were carried out in this work. The first test was to evaluate the ultimate load capacity of the pile. The penetration was stopped at 20, 30, 40, 60 and 80 kg (80 kg is the estimated ultimate load capacity)

compressive loading 5 minutes to read strains at the selected levels along the embedded length, from which load distribution along the pile shaft may be evaluated. The movement of the pile head during loading was measured by means of dial gage fixed at the top of the container from which load settlement relationship may be obtained. The test load was stopped when failure of pile occurred where excessive settlement were measured with little change in the measured load. Finally, the pile was dug out and a new soil specimen was prepared for the second test following the same procedure and conditions used in preparing the first specimen.

In the second test, the pile was loaded to 30 kg compressive load for 15 min, then the pile was subjected to lateral loads normal to its axis, by means of a string passing over a pulley and fixed to the pile cap as shown in Fig.4-1. The lateral loads were applied in 1 kg increments up to 4 kg and the corresponding load deflections at the top of the pile were recorded after 3 minutes of each load increment. Moments along the embedded depth of the pile were measured at 4 kg lateral loading by means of the strain gauges. The loads were then cycled between zero and 4 kg for 10 cycles recording strains at the 5th and 10th cycles.

The lateral loads were then increased to 8 kg in 1 kg increments and the corresponding lateral deflections were recorded. Strains, i.e moments, at 8 kg loading were measured. The loads were cycled 10 times between 4 and 8 kg in one step, deflections were recorded for each cycle and strains were measured at the 5th and 10th cycles. Finally, the horizontal

compressive loading, from which load distributions after applying repetitive lateral loads were obtained. The 30 kg vertical load kept on top of the pile for 12 hours.

In the next day, the vertical load is then increased to 40 kg and the above procedure for lateral loading is repeated except for the 4 kg cyclic loads which was omitted in this stage. The vertical loads were removed and the lateral loads were applied in the same manner 12 hours after the removal of the 40 kg compressive load. The detailed of soil preparation, loading history and the corresponding measurements are given in tables 4-1 and 4-2

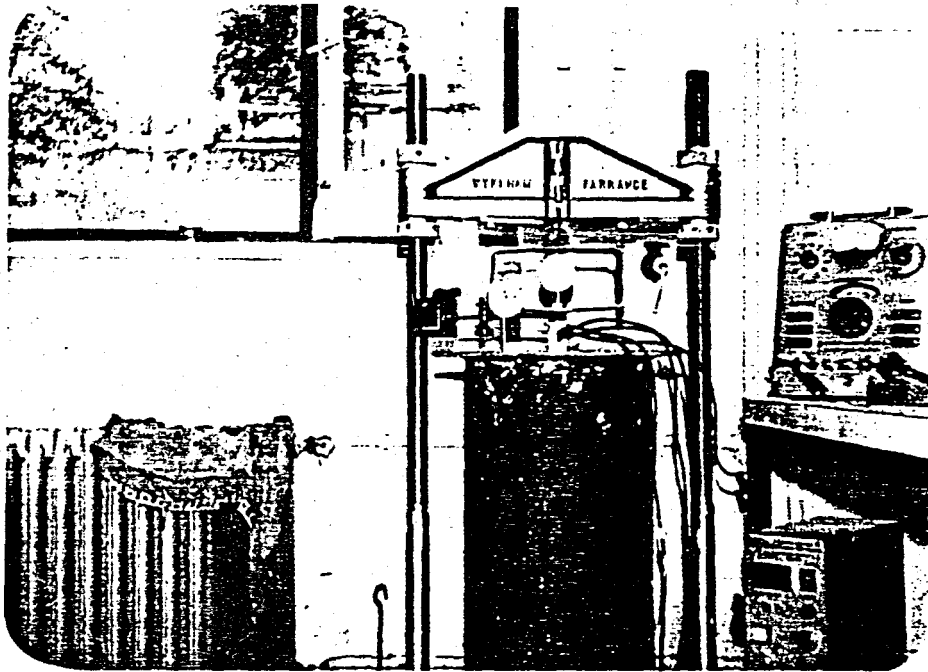


Fig. 4-6 Loading Arrangement

DAY	DETAILS	LOAD STEP	COMP. LOAD	LATERAL LOAD	NO OF CYCLES	MEASUREMENT	REMARKS
1	Mixing the soil at optimum water content						The mixed soil is kept covered in container for 24 hrs
2	compacting the soil at proctor and subjecting it to 2 kg/cm ² pressure						
3	Jacking the pile						The pile is tested after 24 hours of driving
4	Testing the pile to Failure (compression)	1	0-20-40-60-80-0			1-Settlement-load relationship 2-Strains, load distribution	pile is extracted and soil is removed
5	undrained shear strength of soil (undrained - unconsolidated triaxial Test)						C _u value
			END OF TEST NO 1				

Table 4-1 Loading history of Test pile no 1

DAY	DETAILS	LOAD STEP	COMP. LOAD	LATERAL LOAD	NO OF CYCLES	MEASUREMENT	REMARKS
1	as in day 1						
2	as in day 2						
3	as in day 3						
4-A	compressive and lateral loading	2	30	1-2-3-4	1	1-Lateral deflections 2-Strains, moments, at 4 kg	
4-B	compressive and lateral loading	3	30	0-4	10	1-Lateral deflections 2-Strains, moments, at 5 th and 10 th cycles	
4-C	compressive and lateral	4	30	5-6-7-8	1	as in 4-A	
4-D	compressive and lateral	5	30	4-8	10	as in 4-B	
4-E	compressive load	6	30	0	1	Strain (load distribution)	1-Change in load distribution 2-Load is kept for 12 hrs
5-A	compressive and lateral load	7	40	1-2-3-4	1	as in 4-A	

Fig 4-2 Table 4-2 Loading history of test pile no 2

DAY	DETAILS	LOAD STEP	COMP. LOAD	LATERAL LOAD	NO OF CYCLES	MEASUREMENT	REMARKS
5-B	compressive and lateral Load	8	40	5-6-7-8	1	as in 4-A	
5-C	compressive and lateral Load	9	40	4-8	1	as in 4-B	
5-D	compressive Load	10	40	0	10	as in 4-E	
6-A	Lateral Loads	11	0	1-2-3-4	1	as in 4-A	
6-B	Lateral Loads	12	0	5-6-7-8	1	as in 4-A	
6-C	Lateral Loads	13	0	4-8	10	as in 4-B	
7	undrained-unconsolidated Triaxial test					undrained shear strength of soil C_u	

Table 4-2 Cont- loading history of test pile no 2

CHAPTER 5

EVALUATION OF TEST RESULTS

In this chapter, test results obtained from test loads are presented. Results obtained from the compression test loads are discussed first, from which load-settlement relationship and load distributions along the embedded shaft length of various selected loads levels are evaluated.

Lateral load results are then presented from which load-deflections at top of pile, moments distributions and the effect of lateral repetitive loadings on these are discussed.

Finally, the change in stress distributions, due to repetitive lateral loading, along the shaft of pile at 30 kg and 40 kg compressive loads are presented.

5-1 DATA PROCESSING : -**1- LOAD-SETTLEMENT MEASUREMENT : -**

The settlement of the pile is evaluated as the difference between the cell movement, measured by dial indicator placed on top of the cell, and the load gauge indicator mounted on top of the pile cap and fixed to the compression machine frame. The readings of the load gauge is converted to loads in kilograms, using the load gauge calibration table.1

Load-settlement results are given in appendix B, table 2. The load-settlement relationship graph is presented in Fig 5-1.

2 LOAD DISTRIBUTION ALONG THE PILE SHAFT :-

The distribution of the applied load was computed for selected applied load levels from the measured strains in the pile using Hook's law :-

$$E = \frac{\sigma}{\epsilon}$$

or $P = AE \epsilon$ (5-1)

where :-

- A = cross sectional area of pile = 0.1.0 cm²
- E = modulus of elasticity of Alumium = 0.7x10⁶ kg/cm²
- ε = measured strain in 10⁻⁶ inch/inch

subtituting in equation (5-1)

$$P = (1.0) (0.7) (10^6) (10^{-6})$$

$$P = 0.7 \text{ (kg)}$$

measured strains are tabulated in Appendix B, table 3. The load distribution along the shaft is shown in Fig 5-2.

3- MOMENT DISTRIBUTION ALONG PILE SHAFT : -

The measured moments along the shaft of the pile are computed from the measured bending strains caused by lateral loads. The most convenient method to define flextural stiffness as a function of stress level is by the moment - curvature, or $M-\phi$, relationship. The flextural stiffness is equal to the moment divided by the curvature (6) :

$$EI = \frac{M}{\phi} \quad (5-3)$$

Taking :

$$EI = 0.70 \times 10^6 \text{ kg cm}^2$$

$$\phi = \text{measured bending strain} \times 10^{-6}$$

substituting in equation (5-3)

$$M = 0.70 \epsilon \quad (5-4)$$

Measured bending strains due to lateral loads of 4 kg and 8 kg under zero, compressive loading is tabulated in Appendix B, table 4, Fig 5-3 and Fig 5-4 show the distribution of moments along the shaft at different loading conditions.

Dotted lines represent measured values, while the solid line represents the theoretical moment distribution calculated by numerical finite difference method (7) employing the principle of subgrade modulus, the method is presented in Appendix C with

5-2 ANALYSIS OF DATA :

1- LOAD- SETTLEMENT RELATION : -

From load-settlement graph, it is clear that the ultimate load capacity has a value of 82 kg. The corresponding settlement is 0.80 mm which is about 3 % of pile diameter indicating that the pile is behaving as a friction pile. Poulos and Davis have shown that for piles in clay, shaft resistance becomes fully mobilized when the settlement reaches 1 per cent of the shaft diameter. This value has been confirmed experimentally by Whitaker and Cooke (1966) for friction piles in London clay. The 1 per cent settlement in Fig 5-1 corresponds to a load of 68 kg, before this value, the gradient of the curve is almost constant, while after this value, the gradient decreases sharply. It could be concluded that the shaft resistance becomes fully mobilised at 1.0 per cent diameter settlement. Because of the low pile diameter to length ratio, the point resistance, estimated to contribute 15 % of the ultimate load capacity of pile, starts to influence the settlement behaviour of the pile which explains the reduction in slope since the point resistance becomes fully mobilised at higher values of settlement.

The results obtained in this test agree with the previous results obtained by Whitaker and Cooke for piles in London clay.

2- LOAD DISTRIBUTIONS ALONG THE SHAFT : -

The distribution of compressive loads along the pile

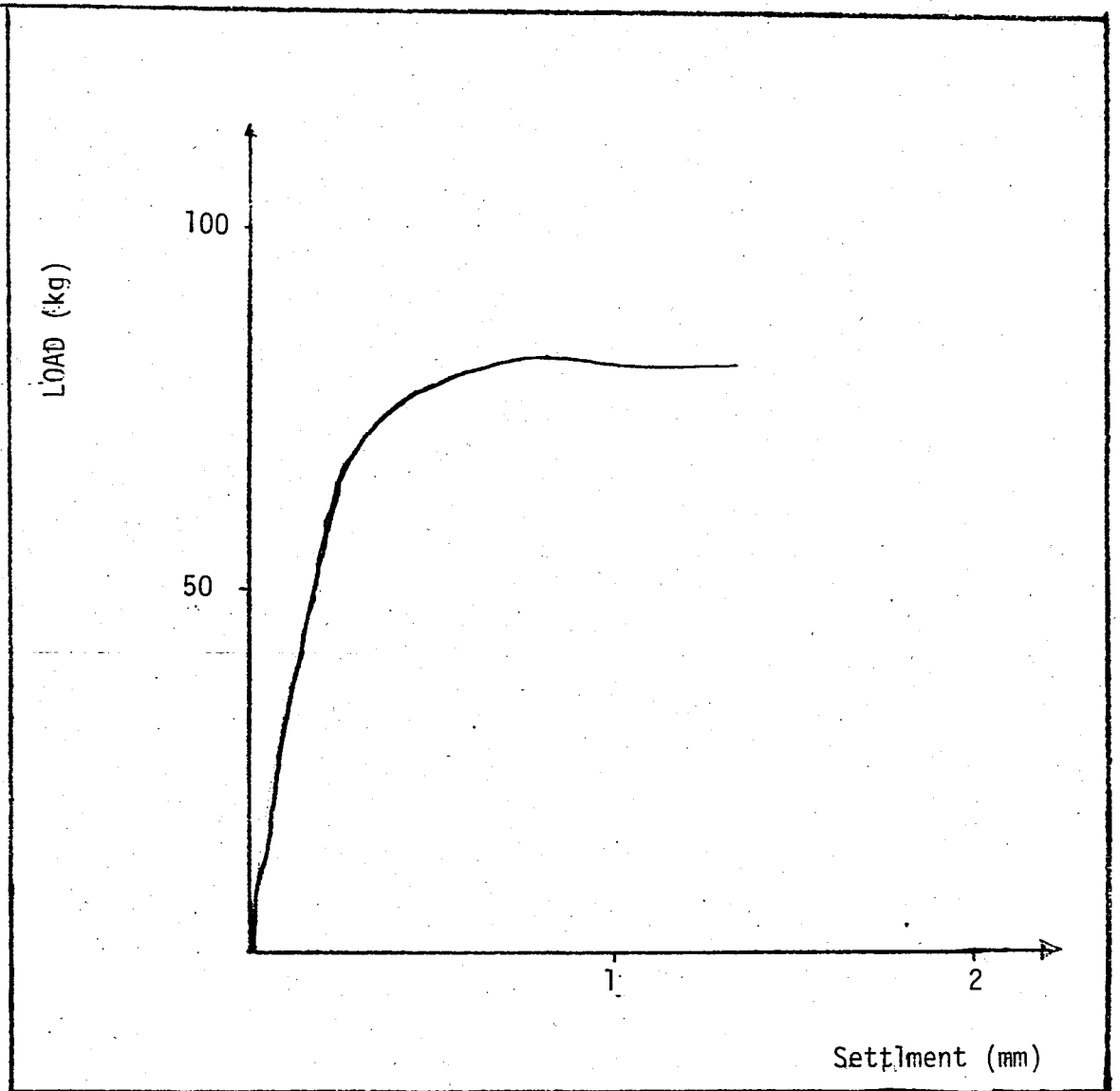


Fig. 5-1 Load-Settlement relationship Graph.

shaft, computed from the compression strains recorded at certain load levels, are plotted in Fig 5-2. Extrapolation of these curves to the pile tip indicates that part of the applied load being carried at the tip of the pile level. The portions of the loads being carried as skin friction and tip resistance at the base level is plotted versus the applied load in Fig 5-3. The difference in the loads at any two-cross sections represents the load carried by friction or adhesion on the surface of the shaft between the two sections "shearing load Transfer". or "load-take". It is evaluated as the slope of the load curves between the chosen sections and given in table 5-1. The variation of the unit skin resistance with depth at 80 kg compressive loading, evaluated as the load transferred at each section divided by the surface area of that section, is given in Fig 5-2A.

THE FOLLOWING POINTS ARE OBSERVED : -

- A- The shape of the load depth curves remains fairly constant as the load increases.
- B- The top section carried less weight, even though it is longer than the other sections, this is because the top soil softens as a result of applied water pressure.
- C- The tip load, offer little contribution to the total load capacity, 10 % of the pile capacity at Failure.
- D- The skin friction at the top of the pile is larger than the skin friction at the bottom of the pile at lower load levels, but as the applied load reaches the failure load, the stress distribution become homogeneous along the pile shaft.

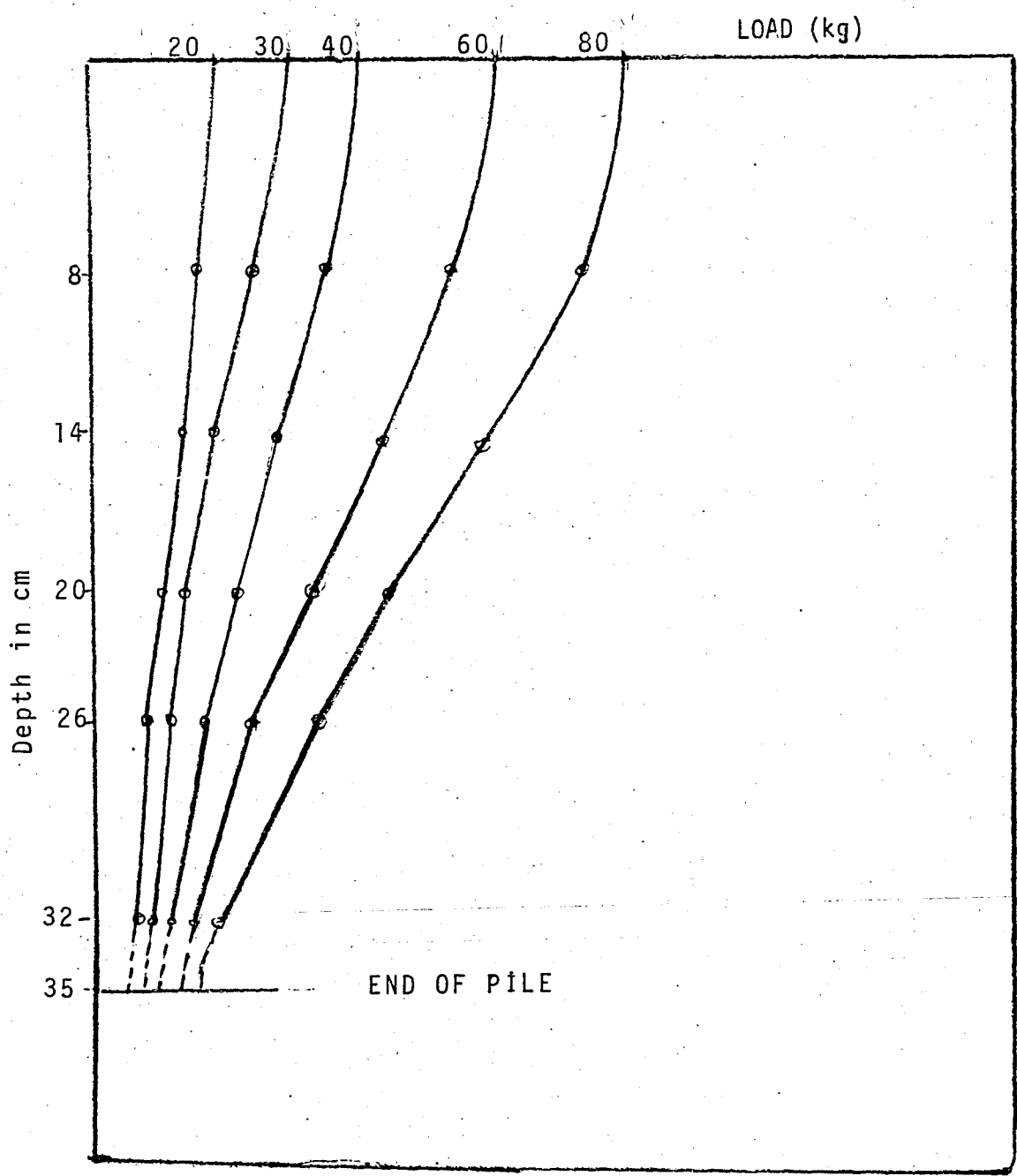


Fig. 5-2 LOAD distribution along the pile.

Unit skin resistance

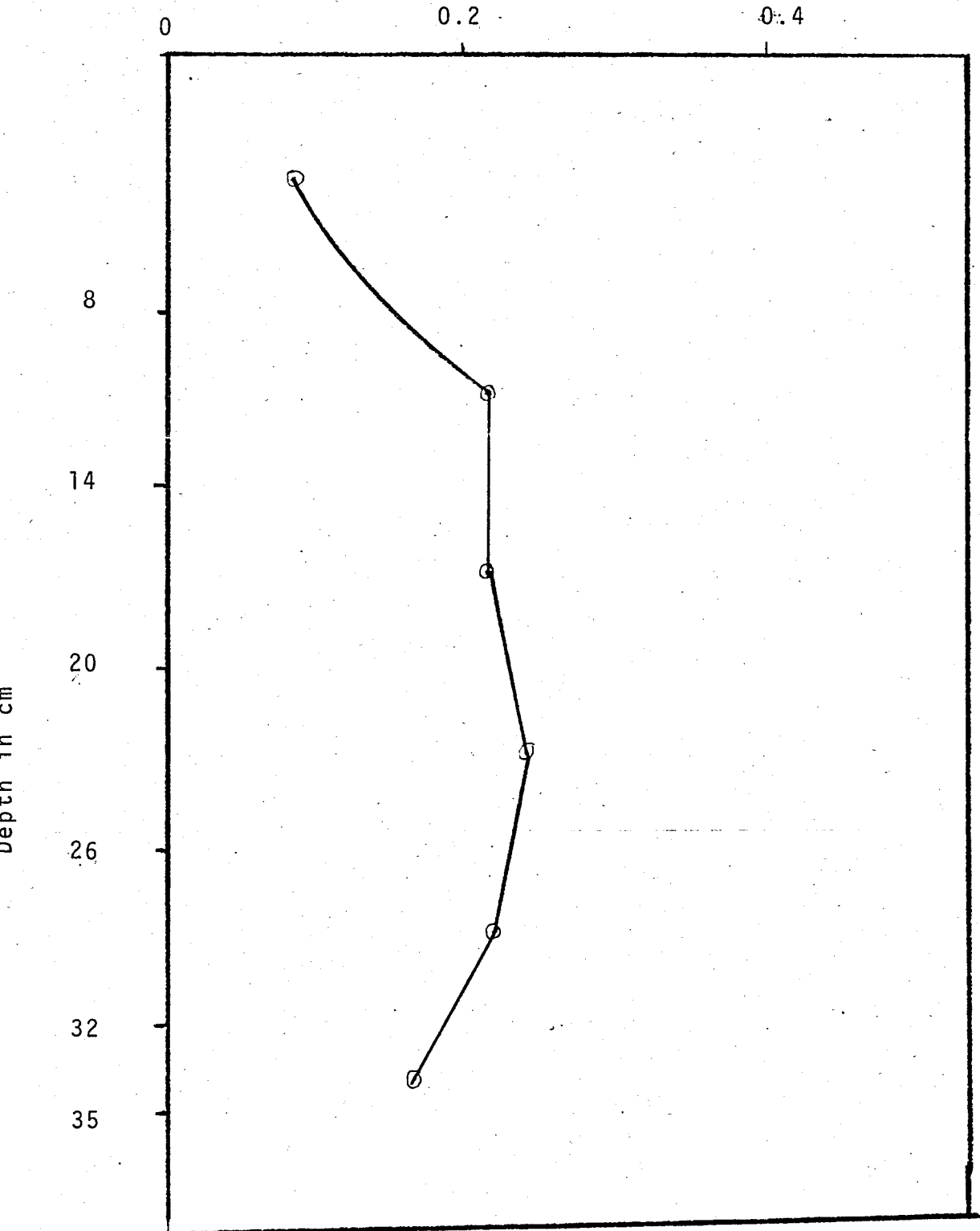


Fig.5-2A variation of unit skin resistance at 80 kg loading

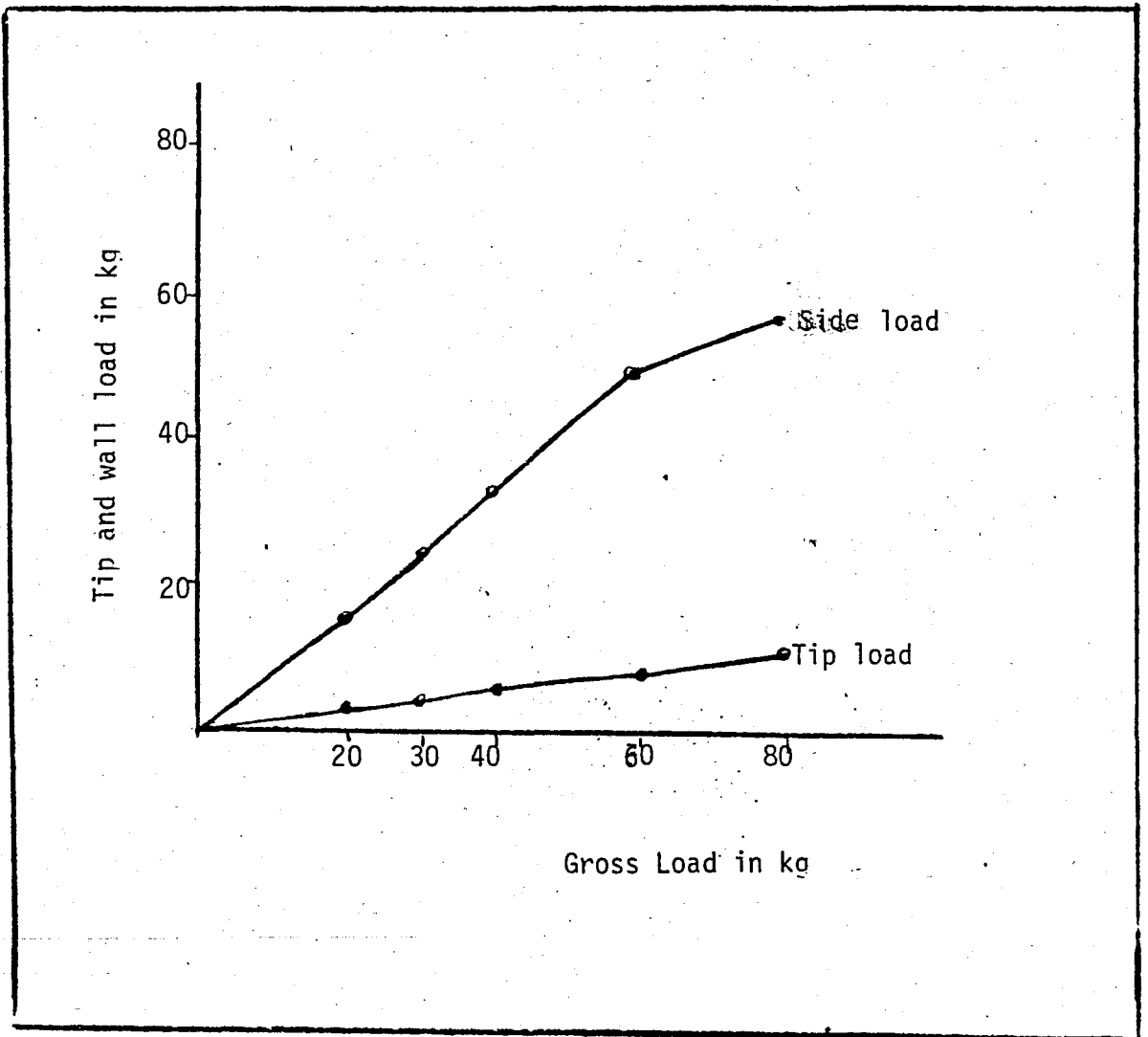


Fig.5- 2 B Loads carried by tip and wall at various loading levels

elev. cm	20	30	40	60	80	Topload
0-8	3.9	5.5	5.7	6.1	7.2	Sideload Friction
8-14	2.8	7	6.3	9.9	13.5	
14-20	3.5	4.9	7.7	12.5	13.5	
20-26	3.5	3.5	6.3	10.5	16.8	
26-32	1.4	1.4	6.3	8.4	13.3	
32-35	6.9	1.5	2.6	4.1	5.1	
	4.0	5.1	8.5	10	11.6	Tipload

Table 5-1 Load carried at each section of Pile

- E- The unit skin resistance, f_s , increases linearly with depth between elevations 0 to 8 cm, while the variation of the unit shearing resistance, f_s , is a constant one from elev 8 cm downward. At elevation 32-35 cm, the value may seem to be less than (0.208), but this could be explained as an error in estimating the tip load by extrapolation.
- F- The adhesion Factor, α , between the pile material and soil may be evaluated from measured unit skin resistance, f_s , and the measured undrained-unconsolidated shear strength of soil, C_u ,

where:

$$" \phi = 0 "$$

$$F_s = C_a = \alpha C_u$$

where

$$f_s = 0.208 \text{ kg/cm}^2$$

$$C_u = 0.2 \text{ kg/cm}^2$$

$$\alpha = \frac{0.208}{0.2} = 1.04$$

which is very close the α value for piles in soft clays.

- G- The bearing capacity factor may be evaluated as follows :

Extrapolated tip load bearing resistance at 80 kg

Tip Load = 11.6 kg

Ultimate load capacity "measured" = 82.5 kg

Since the shaft resistance is fully mobilized at 67 kg, the 2.5 kg difference above will be beared by the tip

$$(Q_{tip})_{ult} = 11.6 + 2.5 = 13.9 \text{ kg}$$

$$(Q_t)_{ult} = C_u N_c A_b$$

Substituting for C_u and A_b by (0.2) and (7-29) respectively, gives

$$N_c = 9.5$$

or:

$$\text{measured } Q_{ult} = 82.5 \text{ kg}$$

$$\text{measured } Q_s = 67.5 \text{ kg}$$

$$\hline Q_t = 14.7 \text{ kg}$$

resulting a value of $N_c = 9.3$

The average of the above two values agrees with $N_c = 9$ used in practical design.

3- LATERAL DEFLECTIONS : -

The lateral deflections at 30 and 40 kg vertical loads are plotted against the lateral load in Fig 5-6. The increase in lateral deflections due to a cyclic loading of 8 kg are shown as dotted lines.

THE FOLLOWING POINTS ARE OBSERVED : -

A- Effect of vertical load :-

Horizontal deflections decrease as the vertical load increases. There is a decrease in lateral deflections of about 43 and 57 percent under 30 kg and 40 kg vertical loads respectively compared with deflections at zero vertical load.

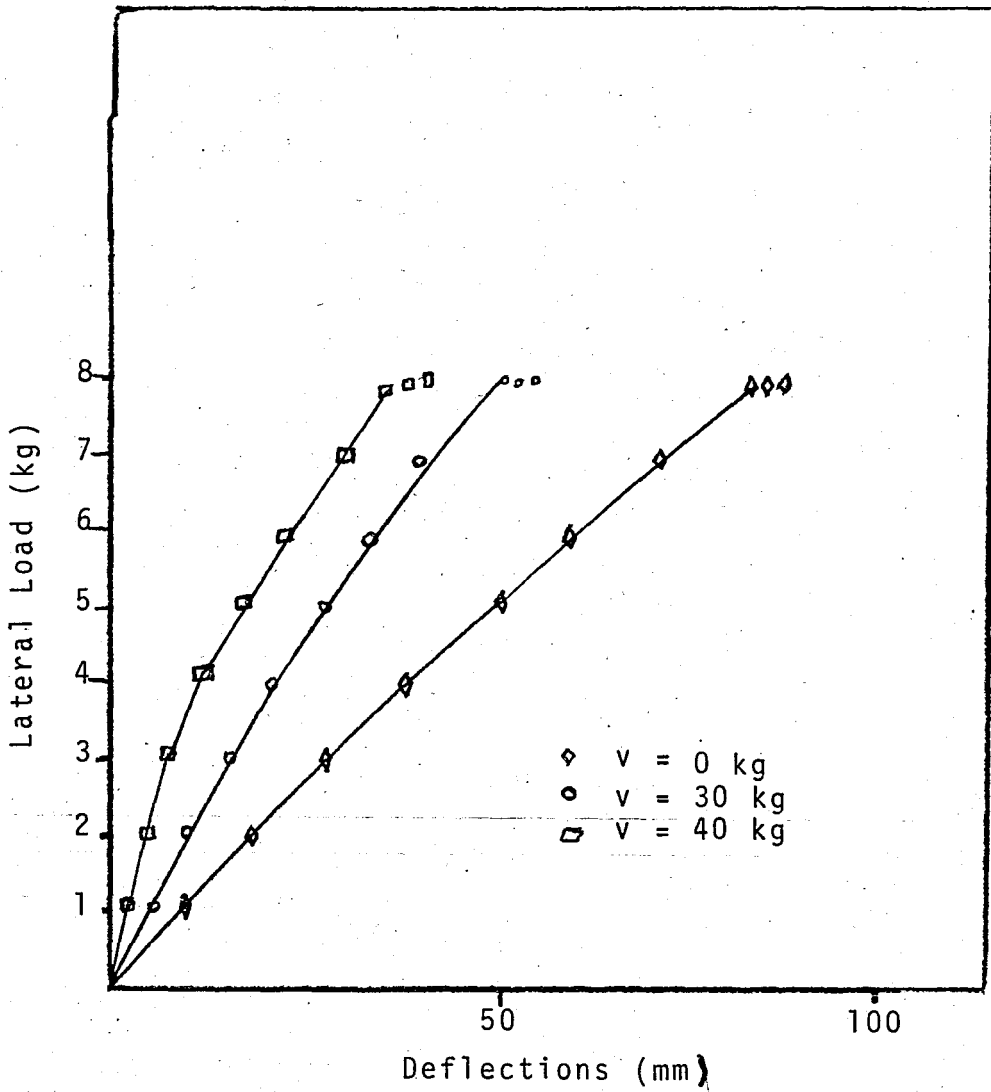


Fig.5-3 Lateral load-deflection graph and the effect of cyclic loading

B- Effect of cyclic loading : -

The measured lateral deflections increased as a result of cycling the lateral load. The increase in deflections by cycling twice between 4 kg and 8 kg were 1 percent under zero vertical load and 6 percent under 30 kg and 40 kg vertical loads.

The increase in deflections after 10 cycles were 5 %, 10 % and 24 % under zero 30 kg and 40 kg compressive loads

4- BENDING MOMENTS :-

The moment along the shaft is determined for each load application from the measured bending strains. The distributions of moments under zero vertical loading are shown in Fig.5-4

THE FOLLOWING POINTS MAY BE CONCLUDED :-

- A- There is an increase in the measured max^m moment of about 76% when the lateral loads has increased from 4 kg to 8 kg.
- B- The depth of the maximum moment has increased when increasing lateral load magnitude.
- C- Cyclic lateral loading did not affect the maximum moment significantly, but caused a large increase in the moment lower portion of the pile.

5- EFFECT OF CYCLIC LATERAL LOAD ON THE LOAD DISTRIBUTION :-

The effect of cyclic lateral loading is demonstrated in Fig.5-6. There is a slight change in the load distribution due to

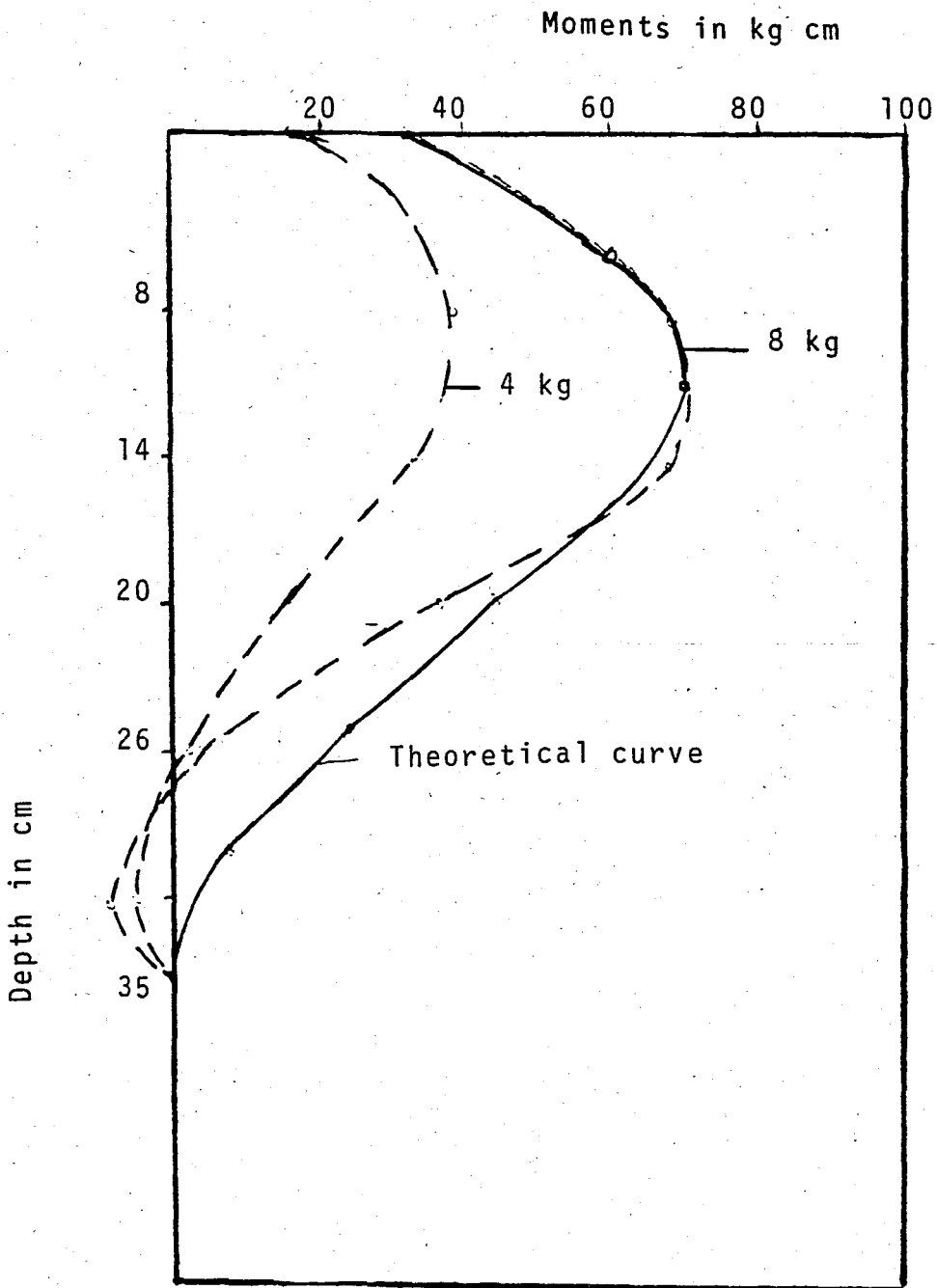


Fig.5-4 Effect of increasing load on Moment

lateral load = 4 kg & 8 kg

vertical load = 0 kg

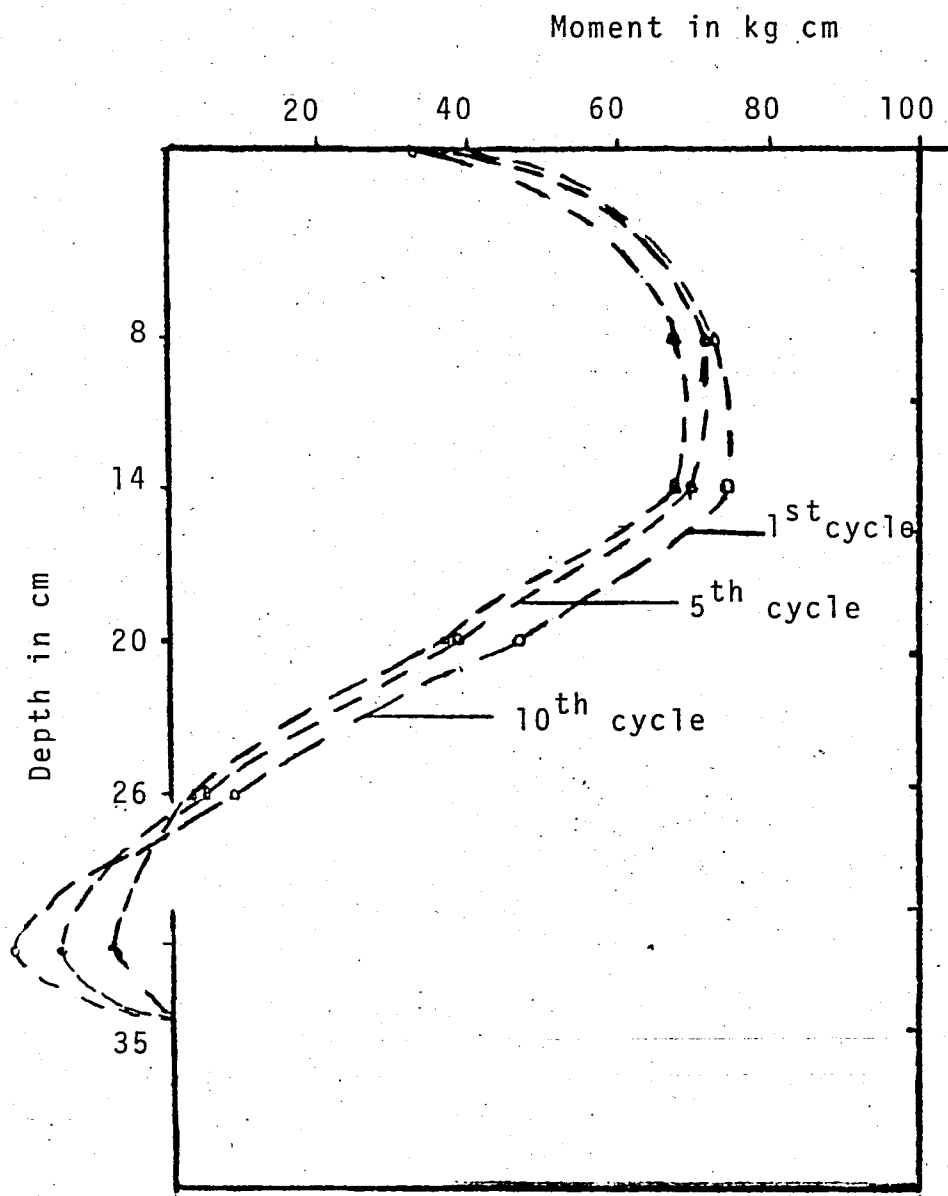


Fig.5-4A Effect of repeated lateral load on Moment

vertical load = 0 kg

lateral load = 8 kg

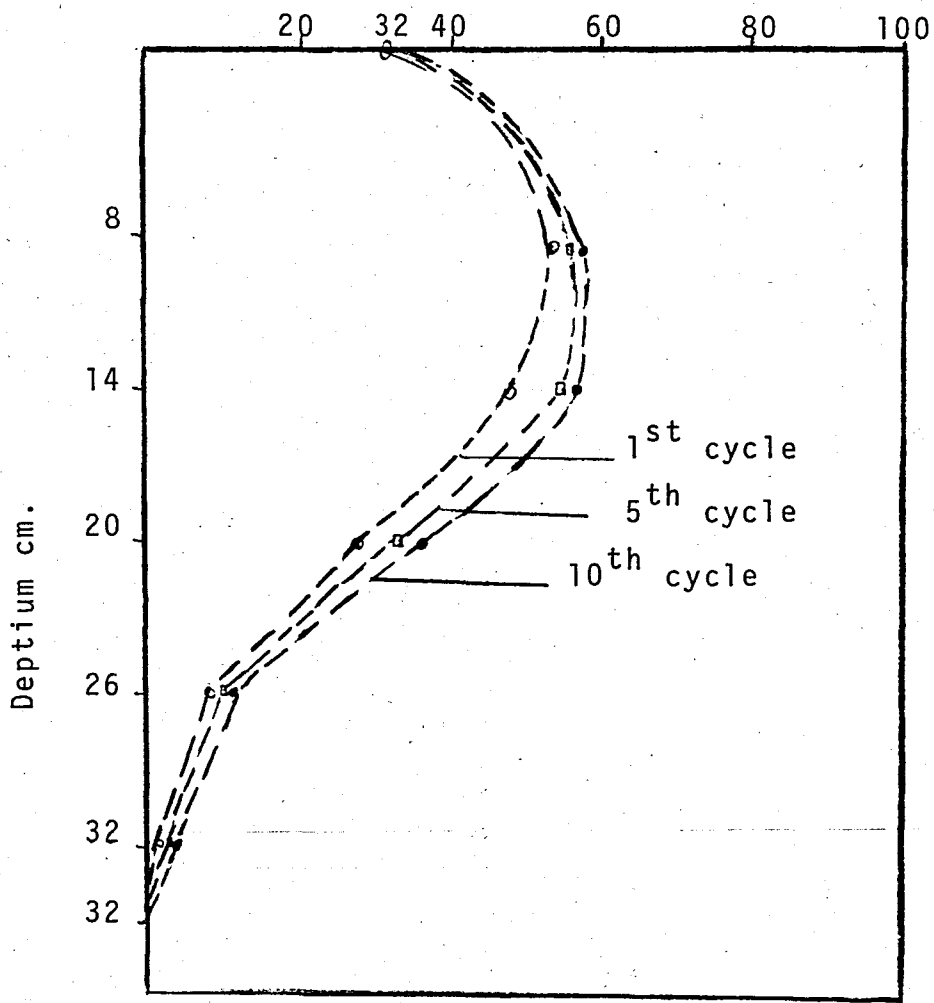


Fig.5-5 Effect of cycling lateral load on Moment

Lateral Load = 8 kg

vertical load = 40 kg

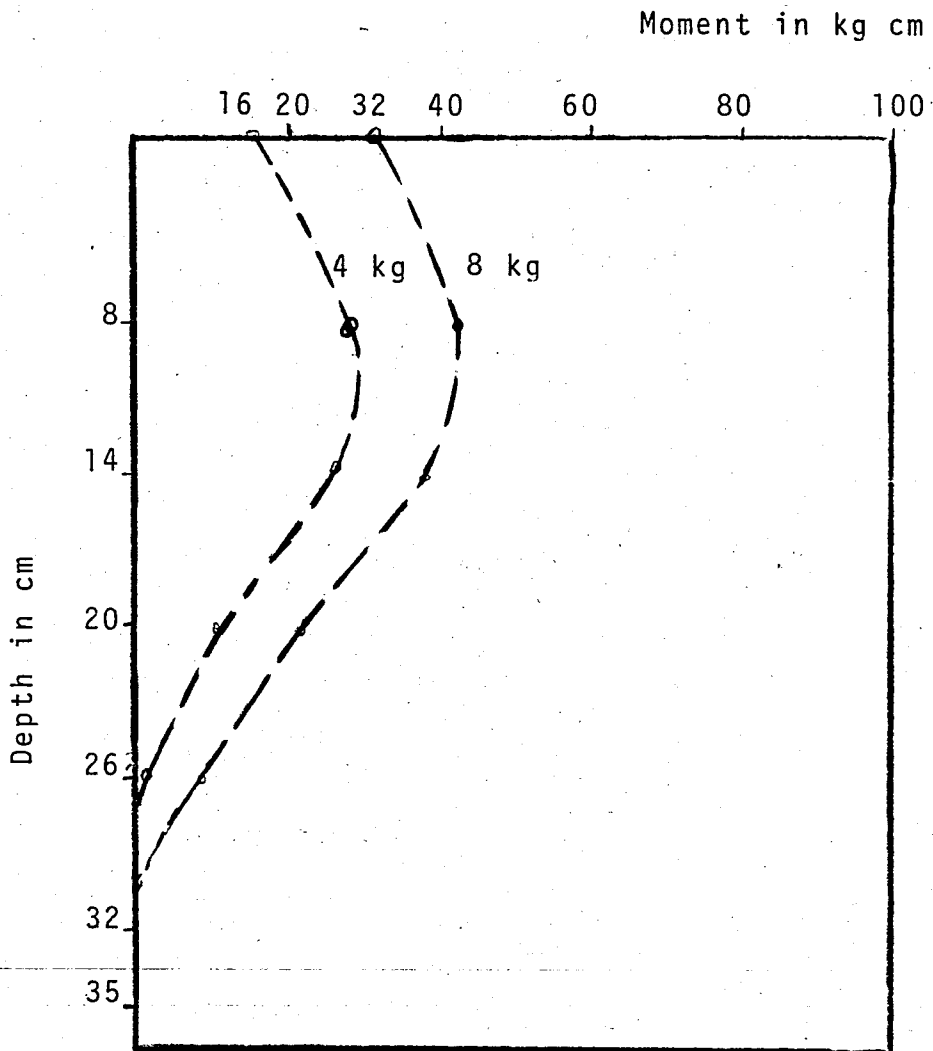


Fig.5- 5A Effect of increasing loads on Moment

vertical load = 30 kg

horizontal load = 4 kg $\frac{1}{2}$ 8 kg

lateral loading. The load carried by the upper section of the pile has decreased, while the load carried by the lower sections and tip has increased. The new load distribution are presented in table 5-2. The new load distribution might have been influenced by residual stress due to lateral loading. The reason for this change is that the soil adjacent to the pile at ground surface yields as a result of lateral loading. In addition, the surface of the pile opposite to the loading direction separates from the soil and, to some depth, leaves a gap, when the load is removed, the contact between the pile's surface and the surrounding soil is not fully recovered due to plastic deformation of the surrounding soil, causing a reduction in the friction resistance of the soil at that section. i.e. a reduction in the "load take-out". The lower sections has to carry this difference in load.

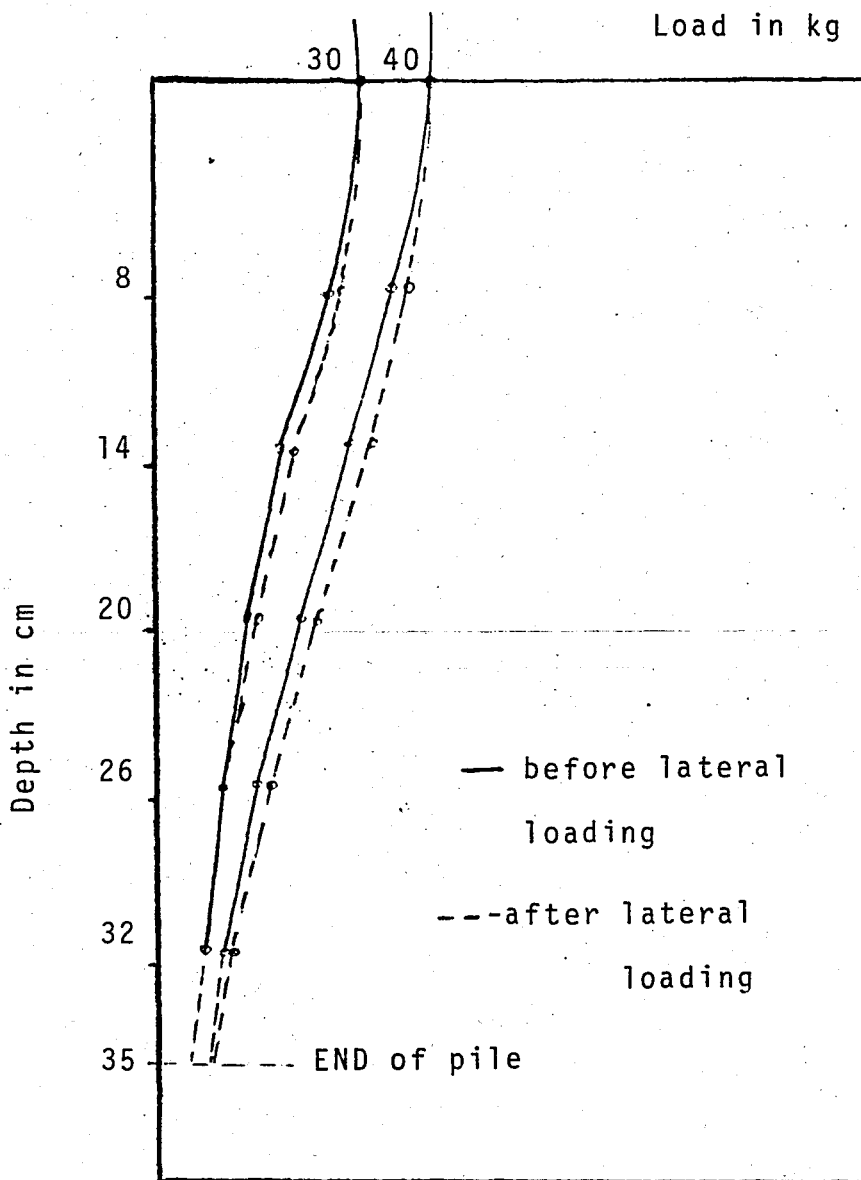


Fig.5-6 Redistribution of load after lateral load applications

before cyclic loading		after cyclic loading		elevation
30	40	30	40	<i>cm</i>
5.5	5.7	3.4	3.4	0-8
7	6.3	6.9	5.4	8-14
4.9	7.7	6.5	8	14-20
3.5	6.3	6.4	7.1	20-26
1.4	6.3	4.1	6.8	26-32
1.5	2.6	2.8		32-35
4.8	5.1			Tip

Table 5-2 Effect of repeated lateral loading on load distribution

CHAPTER 6

SUMMARY AND CONCLUSIONS

In this experimental study, the behaviour of an instrumented friction model pile jacked in clay and subjected to combination of vertical loads as well as lateral loads is investigated. The loading system was designed to simulate a condition such that a single pile loaded vertically with its designed working load is subjected to repetitive lateral loading. An additional vertical load representing an equivalent design over load is introduced, lateral loads were cycled again.

Load-settlement relationship, load transfer along the pile shaft, top deflections and moment distributions along the shaft were measured during the test.

THE FOLLOWING POINTS ARE CONCLUDED :-

- 1- The shaft resistance becomes fully mobilised at about 1 % of pile diameter.
- 2- The shaft resistance offers the major load capacity of the pile ultimate load capacity.
- 3- The shape of the load-depth curve remain fairly similar as the load increases.
- 4- The skin friction at each section of the pile, which is measured from slopes of the load curves, becomes closer in values as the load reaches to failure load.

- 5- The unit shearing stress distributions along the shaft is almost constant, except the top 8 cm.
- 6- An adhesion factor between pile material, Aluminum, and soil of (1) was calculated. This confirms with common practice to take $f_s = C_a = C_u$ for $C_u < 96$ KN
- 7- A value of $N_c = 9$ used in the design is confirmed to be appropriate.
- 8- Vertical loads of 30 kg and 40 kg caused a decrease in lateral deflections of 43 % and 57 % respectively compared with deflections at zero ~~vertical~~ loading
- 9- The measured lateral deflections increased as a result of cyclic lateral loading.
- 10- An increase in max moment of about 75 % is measured when lateral loads increased from 4 kg to 8 kg. The depth of the Maximum moment has increased slightly.
- 11- Repeated loading did not affect the moment significantly, but caused an increase in the negative moment in the lower portion of the pile
- 12- A slight change in the load distribution along the shaft was measured as a result of lateral repeated loading.

REFERENCES

- 1- Poulos,H.G. Davis,E.H. "Pile Foundation Analysis and Design" John Wiley and Sons, Inc, 1980.
- 2- Boroms,B.B., "Design of laterally loaded piles" ASCE,SMFD, Vol 91, No 5M3, pp.79.97, May 1965.
- 3- Whitaker,T. "The Design of Piled Foundations" Pergamon press, 1976.
- 4- Hana,Thomas "Foundation Instrumentation" Trans. Tech Publications, 1973.
- 5- Hoffman,K. "Electrical Measurement of Mechanical Quantites" H.B.M Publications.
- 6- Reese,Lymon C.and Welch,Robert. C. "Lateral loading of deep foundations in Stiff clay" ASCE, vol 101, No GT7, July 1975.
- 7- Smith, G.N.and Pole E.L. "Elements of Foundation Design" Granada Publishing LTD, 1980.
- 8- Cooke,R.W. and Price,G., "Strain and displacement around friction piles" Proc. 8th int. conf.Soil Mech. Moscow vol 2, No 1,pp 53-60.
- 9- Kraft,Fr. Leland M.,Focht A John, A merasinghe,Srinath F. "Friction capacity of piles driven into clay" ASCE, vol.107,No GT 11,Nov 1981 pp 1521-1541
- 10- Fellenius, Bengt H. "Test loading of piles and new proof testing procedure", ASCE, vol 101, No GT 9,September 1975.

- 11- Aurora, Ravi P., Peterson Edward H. "Model study of load transfer in slender pile". Vol 101, June 1975
- 12- Kim Jai B. and Burngraber Robert J. "Full-scale lateral load tests of pile group" Proceedings ASCE, Geotechnical Journal, vol.102, No.GT 1, January 1976
- 13- O'Neill Michael W. "Side load transfer in driven and drilled piles" Proceeding of ASCE, Journal of Geotechnical Engineering vol 108, no. GT 12, December 1982.

APPENDIX A

INITIAL PILE DESIGN

1- Ultimate load capacity :-

The ultimate load capacity is evaluated from equation (2-8) :-

$$(Q)_{ult} = C_u N_c A_b + \alpha C_u A_s$$

$$C_u = 0.20 \text{ kg/cm}^2$$

$$N_c = 9$$

$$\alpha = 1$$

$$A_s = 324 \text{ cm}^2$$

$$A_b = 7.29 \text{ cm}^2$$

$$(Q)_{ult} = (0.2)(9)(7.29) + (1)(0.2)(324)$$

$$(Q)_{ult} = 13.1 + 64.8 = 77.9 \text{ kg.}$$

2- Pile load design load : -

Choose a factor of safety of 2

$$Q = \frac{Q_{ult}}{F.S}$$

$$Q = \frac{75-88}{2} \quad 38 \text{ kg} \quad \text{say } 40 \text{ kg}$$

The above is the maxm working load the pile should be subjected to.

choose

30 kg	working load
<u>10 kg</u>	over load
40 kg	Total working load

NB : The value of factor of safety of 2 is chosen as an extreme value.

3- Lateral loading : -

Building codes allow 10 % of the vertical load capacity of pile for a safe design

$$\text{i.e lateral load} = \frac{76}{10} = 7.6 \quad \text{say 8 kg}$$

From above : -

- 1- The pile will be subjected to 30 kg as normal working load, the load is increased to 40 kg to allow for variation of vertical life load "overload"
- 2- The Max^m lateral load the pile is subjected to is 8 kg.
- 3- Strains are measured at 20,30,40,60, and 80 kg. Load levels.

APPENDIX B

TEST RESULTS

Gauge no 1 (0.01 mm)	Gauge no 2 (0.002 mm)	Pile mov. (mm)	Cell mov. (mm)	real settl. (mm)	real Load (kg)	Remarks
10	33	0.066	0.10	0.034	9.6	Gage 1 cell movement Gage 2 pile movement real settlment:- column 4 - column 3 real load : Load Gage calibration from gage 2
20	66	0.132	0.20	0.068	19.3	
30	99	0.198	0.30	0.102	28.9	
40	132	0.264	0.40	0.136	38.3	
50	165	0.330	0.50	0.170	47.7	
60	204	0.408	0.60	0.192	58.7	
70	-	-	0.70	-	-	
80	249	0.498	0.80	0.302	71.5	
90	257	0.514	0.90	0.386	73.8	
100	268	0.536	1.00	0.464	77.0	
110	275	0.550	1.10	0.550	79.0	
120	285	0.570	1.20	0.630	81.9	
130	291	0.582	1.30	0.718	83.6	
140	298	0.596	1.40	0.804	85.6	
150	285	0.570	1.50	0.93	81.9	
160	285	0.570	1.60	1.03	81.9	
170	287	0.574	1.70	1.126	82.4	

Table B-2 LOAD-Settlement Test result

Load	Gauge No	Strain 10^{-6}	Load	Remarks	
-	Top	-	-	-	
20	1	-23	16.1		
	2	-19	13.3		
	3	-14	9.8		
	4	- 9	6.3		
	5	- 7	4.9		
30	1	-35	24.5		
	2	-25	17.5		
	3	-18	12.6		
	4	-13	9.1		
	5	- 9	6.3		
40	1	-49	34.3		
	2	-32	22.4		(28) extrapolated
	3	-29	20.3		
	4	-20	14		
	5	-11	7.7		
60	1	-77	53.9		
	2	-50	35	(44) extrapolated	
	3	-45	31.5		
	4	-30	21		
	5	-18	12.6		
80	1	-104	72.8		
	2	-66	46.2	(59) extrapolated	
	3	-65	45.5		
	4	-41	28.7		
	5	-22	15.4		

Table B-3 Measured strain along the shaft

lateral Load	cycle	Gauge No	Strain	Moment	Remarks
kg	no	Top	10^{-6}	kgcm	-----
4	1 st	1	55	38.5	
		2	47	32.9	
		3	23	16.1	
		4	3	2.1	
		5	-7	-4.9	
8	1 st	1	98	68.6	
		2	97	67.9	
		3	52	36.4	
		4	4	2.8	
		5	-11	-7.7	
8	5 th	1	103	72.1	
		2	99	69.3	
		3	55	38.5	
		4	+7	4.9	
		5	-21	14.7	
8	10 th	1	102	71.4	
		2	107	74.9	
		3	67	46.9	
		4	12	8.4	
		5	-2.9	-20.3	

Table B-4 Strain readings due to 4 kg and 8 kg lateral loading
vertical load = 0 kg

Lateral Load	Cycle	Gauge No	Strain	Moment	Remarks
kg	no	Top	10^{-6}	kg	---
4	1 st	1	40	28	Gauge no (5) extrapolated
		2	37	25-9	
		3	16	11-2	
		4	2	1-4	
		5	-	-	
8	1 st	1	61	42-7	
		2	55	38.5	
		3	33	22.4	
		4	13	9.1	
		5	-	-	

Table B-4 Strain reading due to 4 kg and 8 kg lateral loading

vertical loading = 30 kg

Lateral Load	Cycle	Gauge No	Strain	Moment	Remarks
kg	no	Top	10^{-6}	kg	_____
8	1 st	1	76	53.2	
		2	69	47.6	
		3	39	27.3	
		4	12	8.4	
		5	2	1.4	
8	5 th	1	77	53.9	
		2	78	54.9	
		3	48	33.6	
		4	11	7.7	
		5	2	1.4	
8	10 th	1	82	57.4	
		2	80	56.0	
		3	52	36.4	
		4	15	10.9	
		5	3	2.1	

Fig. 5-4 Strain readings due to 4 kg, and 8 kg lateral loading

vertical loadign = 40 kg

		Vertical Load			
		30	40	0	
Cycle	Load	Deflections			Remarks
1	1	3.5	0.5	8	
	2	8.5	2	17	
	3	14	5.5	26.5	
	4	20	10	36.5	
	5	26	16	48	
	6	32.5	21	59	
	7	39	28	70.5	
	8	47	36	83	
2	8	50	38	84	
3	8	52	83.5	84	
4	8	52	39	85	
5	8	52	41	85	
6	8	53	41.5	86	
7	8	53	41	86	
8	8	53	41.5	87	
9	8	54	42	87	
10	8	54	44	87.5	

Fig. 5-5 Lateral Load Deflections Results

APPENDIX C (7)

SOLUTIONS OF LATERALLY LOADED PILES USING NUMERICAL FINITE
DIFFERENCE TECHNIQUES

The problem of vertical piles subjected to lateral loading can be solved by finite differences in similar manner to the case of a beam sitting on a winker foundations (Palmer and Thompson, 1948; Gleser (153)). The Theory of this method is given in references (1,7)

If the pile displace throughout its length and to the right Fig C-2, then :-

lateral pressure on R.H.S of pile, $P_p = P'_0 + P$

where $P =$ increase in pressure due to displacement of the pile, Y .

Since

$$P_p = P = K_h y$$

$K_h =$ modulus of horizontal subgrade reaction taken as equal to modulus of vertical subgrade reaction for horizontal beam on the same soil and having a width equal to the pile width.

Boundary conditions : -

Base of the pile : - The bottom of the pile can be displaced and can suffer rotation but it is assumed that no moment develop at the base level.

Top of the pile : The boundary condition at the top of the pile depends upon the form of fixity into the structure it is

supporting. If the pile is fixed then no rotation will develop, but moment will develop. For free headed piles no moment will develop.

It is generally simplest to ignore the boundary conditions at the tip of the pile.

Solution of the test pile : -

Data :

$$K = 1.6 \text{ kg/cm}^2$$

"medium clay"

$$B = 2.7 \text{ cm}$$

$$d = 0.35 \text{ m}$$

$$a = 1 \text{ m}$$

$$E_{AL} = 0.7 \times 10^6 \text{ kg/cm}^2$$

$$H = 8 \text{ kg}$$

$$C = 4 \text{ cm}$$

$$EI = 0.4466 \times 10^6 \text{ kg cm}^2$$

The buried length of the pile is divided into 7 equal section each 5 cm length.

now, refering to Fig C-1

$$Q = q \times \text{Area} = (q) \left(\frac{a}{2} \right) (B) = (k_h)(y) \left(\frac{a}{2} \right) (B)$$

$$Q_1 = 10.8 y_1$$

$$Q_2 = 21.6 y_2$$

$$Q_3 = 21.6 y_3$$

$$Q_4 = 21.6 y_4$$

$$Q_5 = 21.6 y_5$$

$$Q_6 = 21.6 y_6$$

$$Q_7 = 21.6 y_7$$

$$Q_8 = 10.8 y_8$$

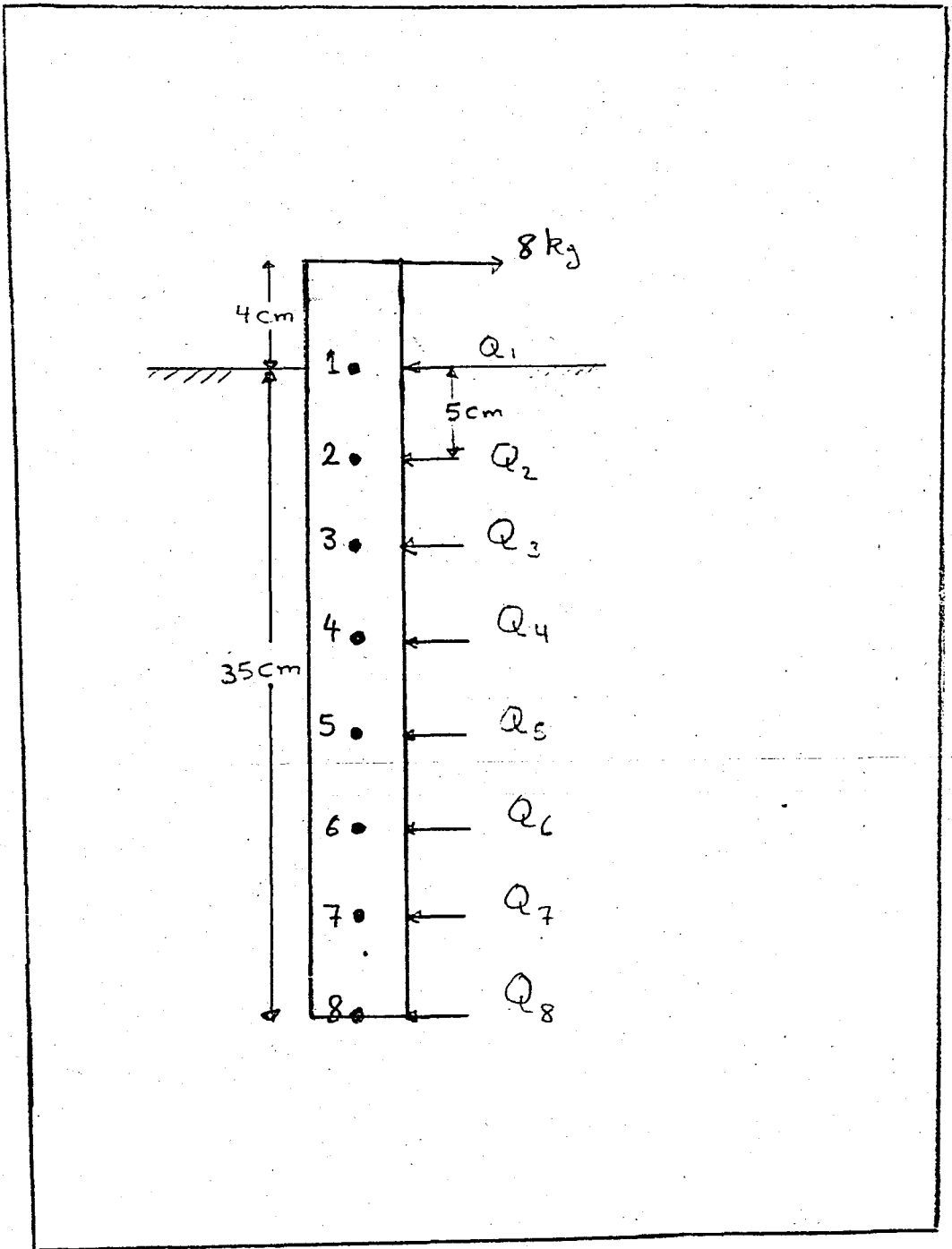


Fig C-1 mode pile Solution by F.D.M

From Beam theory

$$\frac{M}{I} = \frac{E}{R}$$

or
$$-M_i = EI \frac{\delta^2 y_i}{\delta x^2}$$

where:
$$\frac{\delta^2 y_i}{\delta x^2} = \frac{|y_{(i-1)} - 2y_i + y_{(i+1)}|}{a^2}$$

$$-M_i = \frac{446600}{25} |y_{(i-1)} - 2y_i + y_{(i+1)}|$$

$$-M_i = 17864 |y_{(i-1)} - 2y_i + y_{(i+1)}|$$

substituting in the above equation for M_2 to M_6 results in 6 equations with 8 unknowns :-

$$\begin{aligned} (0.997)y_1 - 2y_2 + y_3 &= (4) 10^{-3} \\ -(6.05)(10^{-3})y_1 + 0.994y_2 - 2y_3 + y_4 &= (6.27) 10^{-3} \\ -(9.07)10^{-3} y_1 - (0.012)y_2 + (0.994)y_3 - 2y_4 + y_5 &= (8.5)10^{-3} \end{aligned}$$

$$-0.012y_1 - 0.018y_2 - 0.012y_3 + 0.994y_4 - 2y_5 + y_6 = -0.011$$

$$-0.015y_1 - 0.024y_2 - 0.018y_3 - 0.012y_4 + 0.994y_5 - 2y_6 + y_7 = -0.013$$

$$-0.018y_1 - 0.030y_2 - 0.024y_3 - 0.018y_4 - 0.012y_5 + 0.994y_6 - 2y_7 + y_8 = -0.015$$

From B.C. :

At the Bottom $M_8 = 0$ ==

$$378y_1 + 684y_2 + 540y_3 + 432y_4 + 324y_5 + 216y_6 + 108y_7 = 312$$

Equilibrium of factors $R = 0$ ==

$$10.8y_1 + 21.6y_2 + 21.6y_3 + 21.6y_4 + 21.6y_5 + 21.6y_6 + 21.6y_7 + 10.8y_8 = 8$$

Arranging in Matrix form and solving the 8x8 Matrix with a programmable calculator using Gauss elimination, displacements, shear and moments at points. 1 to 8 are found. Fig C-2

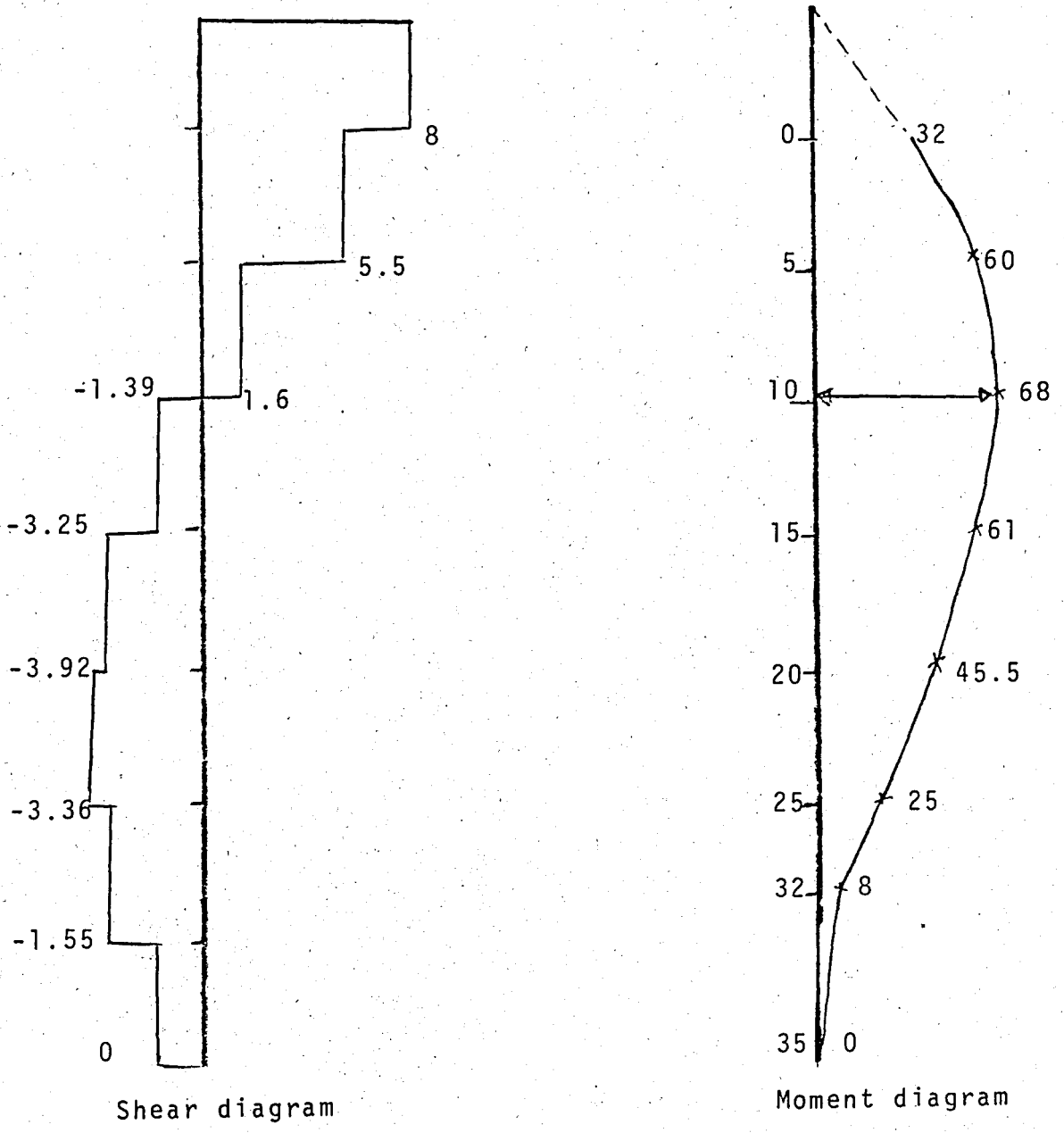


Fig C-2 Shear and Moment diagram evaluated by Finite difference method